Transmit Codes and Receive Filters for Pulse Compression Radar Systems

Petre Stoica[†], Jian Li[‡], and Ming Xue[‡]

Abstract

Pulse compression radar systems make use of transmit code sequences and receive filters that are specially designed to achieve good range resolution and target detection capability at practically acceptable transmit peak power levels. The present paper is a contribution to and a survey of the literature on the problem of designing transmit codes and receive filters for radar. In a nutshell: the main goal of this paper, which considers the cases of both negligible and non-negligible Doppler shifts, is to show how to design the receive filter (including its length) and the transmit code sequence via the optimization of a number of relevant metrics considered separately or in combination. The paper also contains several numerical studies whose aim is to illustrate the performance of the presented designs. Compared with most of the previously published works on the subject, the present contribution is more coherent as well as more complete, and yet the approach taken here is generally simpler both conceptually and computationally. Finally, we remark on the fact that while the focus of this paper is on radar systems, for the sake of being specific, the theory and design methods presented should be useful to several other active sensing applications, such as sonar, non-destructive testing, seismic exploration, and biomedical imaging.

Technical Report 2007-12-03[1]
Department of Electrical and Computer Engineering
University of Florida, P. O. Box 116130, Gainesville, FL 32611

December, 2007

This work was supported in part by the Office of Naval Research under Grant No. N000140710293, the Army Research Office under Grant No. W911NF-07-1-0450, the Defense Advanced Research Projects Agency under Grant No. HR0011-06-1-0031, the National Science Foundation under Grant No. CCF-0634786, the Swedish Research Council (VR) and the European Research Council (ERC). Opinions, interpretations, conclusions, and recommendations are those of the authors and are not necessarily endorsed by the United States Government.

[†]Petre Stoica is with the Department of Information Technology, Uppsala University, Uppsala, Sweden. Phone: 46-18-471.7619; Fax: 46-18-511925; Email: ps@it.uu.se.

[‡]Jian Li and Ming Xue are with the Department of Electrical and Computer Engineering, University of Florida, Gainesville, FL 32611-6130, USA.

[1]Please address all correspondence to: Dr. Jian Li, Department of Electrical and Computer Engineering, P. O. Box 116130, University of Florida, Gainesville, FL 32611, USA. Phone: (352) 392-2642. Fax: (352) 392-0044. E-mail: li@dsp.ufl.edu.

I. Introduction and Preliminaries

Possible applications of the theory and methods presented in this paper are in active sensing as used in radar, sonar, non-destructive testing, seismic exploration, and biomedical imaging. For the sake of being specific, in the following we focus on the radar application.

Improving the range resolution and target detection capability of a radar system can be done by decreasing the width of the probing pulse and increasing the transmitted energy. However, doing so leads inevitably to large transmit peak power levels that are unacceptable in most systems. Pulse compression is an approach widely used to circumvent the large power peak problem. In this approach, a relatively long train of modulated subpulses is transmitted towards the area of interest. The said subpulses may be rectangular or they may have a different shape – we will not be concerned with the subpulse design in this paper. In any case, the subpulse train will have a much smaller peak power than a single pulse, at the same total transmitted energy.

Let N denote the number of subpulses and let $\{s_n\}_{n=1}^N$ be the modulating code sequence. The signal that arrives at the receiver of the radar system is first demodulated (by means of subpulse matched filtering) and then analog-to-digital converted. The so-obtained received sequence can be modelled as follows. Let $\{y_n\}_{n=1}^N$ denote a segment (or window) of the received sequence, which is temporally aligned with the return from the range bin of interest. Then under some mild conditions (see Equation (6) below), we can write $\{y_n\}$ as (see, e.g., [1]–[4]):

$$\begin{aligned}\begin{bmatrix} y_1 \\ y_2 \\ \vdots \\ y_N \end{bmatrix} &= \alpha_0 \begin{bmatrix} s_1 \\ s_2 \\ \vdots \\ s_N \end{bmatrix} + \alpha_1 \begin{bmatrix} 0 \\ s_1 \\ \vdots \\ s_{N-1} \end{bmatrix} + \cdots + \alpha_{N-1} \begin{bmatrix} 0 \\ \vdots \\ 0 \\ s_1 \end{bmatrix} \\ &\quad + \alpha_{-1} \begin{bmatrix} s_2 \\ \vdots \\ s_N \\ 0 \end{bmatrix} + \cdots + \alpha_{-N+1} \begin{bmatrix} s_N \\ 0 \\ \vdots \\ 0 \end{bmatrix} + \begin{bmatrix} \epsilon_1 \\ \epsilon_2 \\ \vdots \\ \epsilon_N \end{bmatrix}, \end{aligned} \tag{1}$$

where $\{\epsilon_n\}$ denote the noise samples, $\{\alpha_k\}$ are complex-valued scalars proportional to the radar cross sections (RCS's) of the range bins illuminated by the radar system, and α_0 corresponds to the range bin of current interest. Obviously, equations similar to (1) can be written for other range bins, e.g., corresponding to α_1, α_{-1}, etc., by picking up the right segment (or sliding window) of the received sequence. Note that Equation (1)

is a special case of Equation (6) presented in the next section, and so the same conditions as detailed in the following section are required for both (1) and (6) to hold. Also, note that (1) assumes that there is no Doppler shift. This assumption, which does not hold when some targets illuminated by the radar are rapidly moving with unknown directions and velocities, will be relaxed in Section IV.

Remark: The model (1) can be re-written as a convolution sum:

$$y_n = \sum_{k=-N+1}^{N-1} \alpha_k s_{n-k} + \epsilon_n, \quad n = 1, \cdots, N, \tag{2}$$

where $s_k = 0$ for $k \notin [1, N]$. Equivalently, we can write (2) as:

$$y_n = \sum_{k=1}^{N} s_k \alpha_{n-k} + \epsilon_n, \quad n = 1, \cdots, N. \tag{3}$$

The above convolution sum-based models are sometimes used in lieu of (1) (see, e.g., [4]–[6]). However, for our purposes in this paper, the form (1) of the model is more convenient. □

A main problem of the radar's signal processor is to estimate the RCS parameters $\{\alpha_k\}$ from the observations $\{y_n\}$, and to detect which ones of these RCS's can be considered to take on "significant" values. One can see, for instance from (1), that this is not an easy problem: in particular, note that the number of unknowns $\{\alpha_k\}$ in (1) is larger than the number of observations $\{y_n\}$. In coded pulse compression systems, one of the most commonly used methods for estimating the RCS's is based on matched filtering (MF):

$$\hat{\alpha}_0 = \frac{\sum_{n=1}^{N} s_n^* y_n}{\sum_{n=1}^{N} |s_n|^2}, \tag{4}$$

where $(\cdot)^*$ denotes the conjugate transpose for matrices and the complex conjugate for scalars. Evidently, this is nothing but the least-squares estimate of α_0 in (1), which has good statistical properties only if the vector multiplying α_0 in (1) is (nearly) orthogonal to the other vectors in that equation; mathematically this condition can be expressed as:

$$\frac{|\sum_{n=1}^{N} s_n^* s_{n-k}|}{\sum_{n=1}^{N} |s_n|^2} \ll 1, \quad \text{for } k = -N+1, \cdots, -1, 1, \cdots, N-1. \tag{5}$$

where $s_k = 0$ for $k \notin [1, N]$. Whenever (5) holds true, the MF-based receiver achieves nearly perfect pulse compression (that is to say, the output of the said receiver resembles the signal received by a system that transmits a single pulse).

Sequences $\{s_n\}$ that are coded in both phase and amplitude offer most flexibility for satisfaction of (5). However, such sequences are not common in practical systems due to the high cost of providing amplitude

modulation. Typically, the current radar systems use phase-coded sequences, quite often binary sequences, which are easy to generate in a radar transmitter. In this paper, particularly in its numerical case studies, we will focus on the cases in which $\{s_n\}$ is a binary sequence that takes on the values ± 1. However, most of the results, methods, and discussions in the following hold for *arbitrary* code sequences $\{s_n\}$.

There is a considerable literature on designing binary sequences with "good" correlation properties that satisfy (5), see, e.g., [7] and [8] for recent reviews of this literature. Nevertheless, there is no known binary sequence for which the ratio in (5) takes on satisfactorily small values; indeed, for such sequences the smallest known squared value of the said ratio corresponds to a Barker sequence of length $N = 13$ and it is given by $1/(14.083)^2 = -22.974$ dB – such a value would be unacceptably high for many practical applications.

The so-called mismatched filtering (MMF) is a pulse compression approach whose interference (clutter) cancelation performance can be better than that of MF by several orders of magnitude. The rich literature on MMF, of which the references [1]–[4], [9]–[20] of this paper form a representative sample, is briefly discussed in the next section, which also states the problems to be dealt with in the paper.

II. Problem Formulation and Outlook

The radar system is assumed to use the same modulating sequence as before, $\{s_n\}$, but now the received data vector used to estimate the RCS's in a one-by-one fashion has length $2M + N$ instead of just N as in (1), with the integer M being a design parameter. Let $\{y_n\}_{n=1}^{2M+N}$ denote the window of the received data sequence that is temporally aligned with the return from the range bin of current interest. Then, under the usual assumption that the pulse repetition interval (PRI) is large enough such that any return due to the previous transmitted pulse arrives at the receiver before the returns due to the current pulse, we can write the model for

the aforementioned data window in the following form:

$$\begin{bmatrix} y_1 \\ \vdots \\ y_{2M+N} \end{bmatrix} = \alpha_0 \begin{bmatrix} \mathbf{0}_M \\ s_1 \\ \vdots \\ s_N \\ \mathbf{0}_M \end{bmatrix} + \alpha_1 \begin{bmatrix} \mathbf{0}_{M+1} \\ s_1 \\ \vdots \\ s_N \\ \mathbf{0}_{M-1} \end{bmatrix} + \cdots + \alpha_{M+N-1} \begin{bmatrix} \mathbf{0}_{2M+N-1} \\ s_1 \end{bmatrix}$$

$$+\alpha_{-1} \begin{bmatrix} \mathbf{0}_{M-1} \\ s_1 \\ \vdots \\ s_N \\ \mathbf{0}_{M+1} \end{bmatrix} + \cdots + \alpha_{-M-N+1} \begin{bmatrix} s_N \\ \mathbf{0}_{2M+N-1} \end{bmatrix} + \begin{bmatrix} \epsilon_1 \\ \vdots \\ \epsilon_{2M+N} \end{bmatrix}, \tag{6}$$

where $\mathbf{0}_M$ denotes an $M \times 1$ all-zero vector. Let

$$\mathbf{J}_n = \begin{bmatrix} \overbrace{\qquad\qquad}^{n+1} & & \\ & 1 & \mathbf{0} \\ & & \ddots \\ & & 1 \\ & & \\ & \mathbf{0} & \end{bmatrix} = \mathbf{J}_{-n}^T, \quad n = 1, \cdots, M+N-1 \tag{7}$$

denote the $(2M+N) \times (2M+N)$ shift matrix, and let

$$\mathbf{s} = \begin{bmatrix} \mathbf{0}_M^T & s_1 & \cdots & s_N & \mathbf{0}_M^T \end{bmatrix}^T, \tag{8}$$

where $(\cdot)^T$ denotes the transpose. Using this notation, we can write (6) in a more compact manner:

$$\mathbf{y} = \alpha_0 \mathbf{s} + \sum_{k=-M-N+1, k\neq 0}^{M+N-1} \alpha_k \mathbf{J}_k \mathbf{s} + \boldsymbol{\epsilon}, \tag{9}$$

where the vectors $\mathbf{y}$ and $\boldsymbol{\epsilon}$ are defined in an obvious way. In this paper, we assume that the noise sequence is white so that

$$E\{\boldsymbol{\epsilon}\boldsymbol{\epsilon}^*\} = \sigma^2 \mathbf{I}, \tag{10}$$

where $E\{\cdot\}$ denotes the expectation operator. The model equation above is written in a general form that will be used in this paper mostly to motivate the performance metrics employed for code sequence and receiver filter designs. In some cases, Equation (9) could be written in a simplified form; for instance, for the range

bins near (or far away from) the radar system, α_1, α_2, etc. (α_{-1}, α_{-2}, etc.) might be known to be equal to zero. However, for operational simplicity, we will consider the same designed receiver filter and, of course, code sequence for all range bins in the area illuminated by the radar system, and consequently we will use the general model in (9) for all these range bins.

Remark: In (8), the same numbers of zeros precede and, respectively, succeed the code sequence $\{s_n\}$. While there is no strong rationale for this "symmetry" of (8), we use it to simplify the discussion. Note that if the said numbers were different, then we would have two design parameters instead of one (i.e., M), and this fact would complicate the notation and the design procedure without offering any guarantee for a consistently better performance. □

There is an immediately apparent advantage of the extended model in (6) over that in (1). For (1), the ratio between the number of unknowns and the number of observations is given by:

$$\frac{2N-1}{N}, \tag{11}$$

which is approximately equal to 2 for reasonably large values of N. On the other hand, the same ratio for (6) is equal to:

$$\frac{2M+2N-1}{2M+N}, \tag{12}$$

which is close to 1 for $M \gg N$. This simple observation lends some (preliminary) support to the fact that we should indeed prefer (6) over (1).

In order to have $M \gg N$, we should in principle keep N relatively small (otherwise choosing $M \gg N$ might not be possible, as $2M+N$ should in general be only a fraction of the PRI). On the one hand, using a relatively small value of N is an advantage because it allows us to solve the problem of designing $\{s_n\}_{n=1}^N$ more easily (the computational complexity of this problem increases exponentially with N). On the other hand, short code sequences may be more easily identified and thus their use may increase the probability of intercept – unless we will avoid using standard sequences (such as Barker codes), which is what we recommend to do (see the above comment on designing $\{s_n\}_{n=1}^N$, and the next sections) whenever the probability of intercept is an important parameter. Note also that "too short" code sequences may have poor RCS (and Doppler) estimation capabilities.

The following discussion provides further arguments in the favor of (6). If there were no interference terms in (6) (i.e., $\alpha_k = 0$ for any $k \neq 0$), then the MF estimate of α_0 would have excellent statistical properties;

note that the MF estimates of α_0 obtained from (1) and from (6) are identical. However, the no-interference condition mentioned above is never satisfied in practice. Consequently, in an attempt to obviate the need for this condition, we will consider a more general method for estimating α_0, which we call the *instrumental variable (IV) method* and which includes the MF method as a special case. The IV estimate of α_0 is given by:

$$\hat{\alpha}_0 = \frac{\mathbf{x}^*\mathbf{y}}{\mathbf{x}^*\mathbf{s}}, \tag{13}$$

where $\mathbf{x}$ is a $(2M+N)\times 1$ vector of "instrumental variables" (clearly, (13) reduces to the MF-estimate of α_0 for $\mathbf{x}=\mathbf{s}$). We will comment on the terminology used (IV etc.) shortly. However, before doing so, we make a number of remarks on (13), the corresponding MF estimate, and the advantage of using (6) with (13), in lieu of using (1).

Evidently, (13) is more complex computationally than the MF estimate of α_0: in particular, while the latter estimate does not require any multiplication (in the case of binary $\{s_n\}$), the IV estimate needs $(2M+N)$ multiplies. However, most modern radar processors are powerful enough to handle (13) easily, and hence the higher computational requirement of (13) cannot be considered to be a serious drawback. As a matter of fact, the higher computational complexity of (13) is completely offset by the statistical performance advantage of (13) over the MF estimate. To realize the said advantage, the reader is reminded that the MF estimate of α_0 is not significantly affected by the interference terms in (1) or (6) only if the condition (5) is satisfied. Finding a sequence $\{s_n\}$ that satisfies this condition is evidently difficult, as $\{s_n\}$ are constrained to be binary. On the other hand, for the IV estimate the similar condition is that $\mathbf{x}$ is nearly orthogonal to the vectors in (1) or (6) that multiply α_k for any $k\neq 0$ (see below for details). Because the elements of $\mathbf{x}$ are not constrained in any way, satisfying this condition should be an easier task. Moreover, the number of degrees of freedom that can be used for realizing this task increases as M increases, an observation that provides further support to the fact that the extended model in (6) is preferable to (1).

The use of the IV estimate in pulse compression radar systems was apparently suggested several decades ago, see, e.g., [1]–[3], [15], [16], [18]–[20] and the references therein, under the name of mismatched filtering (MMF). In our opinion, the MMF terminology, used in the cited works, is not entirely appropriate: first, the name of MMF has a negative connotation, which might suggest that this filter is somehow incorrect or at least worse than the MF (whereas the opposite is in general true); second, and perhaps more important, the optimal IV vector $\mathbf{x}$ is quite tied/matched to $\mathbf{s}$, even though not equal to $\mathbf{s}$ (see the next section), and thus it does not seem right to call it "mismatched." For these reasons, we will use the name of IV to designate the approach

based on (13) and the quantities involved. The motivation for this name comes from the fact that the elements of the IV vector $\mathbf{x}$, unlike those of $\mathbf{s}$, do not necessarily have a "physical meaning": they are just "instruments" that help us achieve the goal of estimating $\{\alpha_k\}$ accurately (see [21] and the references there for more details on this aspect).

Our main problem in this paper is to choose the user's parameters $\mathbf{x}$, M, and $\mathbf{s}$ in such a way that the estimation errors in $\hat{\alpha}_0$ are minimized. We will consider only data-independent designs for these user's parameters, based on the following metrics:

- Integrated sidelobe level (ISL):

$$\text{ISL} = \frac{\sum_{k=-M-N+1, k\neq 0}^{M+N-1} \left|\mathbf{x}^* \mathbf{J}_k \mathbf{s}\right|^2}{\left|\mathbf{x}^* \mathbf{s}\right|^2}. \tag{14}$$

- Peak sidelobe level (PSL):

$$\text{PSL} = \max_k \frac{\left|\mathbf{x}^* \mathbf{J}_k \mathbf{s}\right|^2}{\left|\mathbf{x}^* \mathbf{s}\right|^2}, \quad \text{for } k = -M-N+1, \cdots, -1, 1, \cdots, M+N-1. \tag{15}$$

- Inverse signal-to-noise ratio (ISNR):

$$\text{ISNR} = \frac{\|\mathbf{x}\|^2}{\left|\mathbf{x}^* \mathbf{s}\right|^2}. \tag{16}$$

  where $\|\cdot\|$ denotes the Euclidean norm.

Note that we have formulated these metrics for complex-valued variables, for the sake of generality. However, when $\mathbf{s}$ is real-valued (as assumed in some parts of this paper), then $\mathbf{x}$ should also be chosen to be real-valued. Our goal is to select the design variables $\mathbf{x}$, M, and $\mathbf{s}$ so that the above metrics are minimized, or at least so that they take on some specified values. In this way, we guarantee that $\hat{\alpha}_0$ in (13) is an accurate estimate of α_0. To see why this is so, insert (9) in (13) to obtain:

$$\hat{\alpha}_0 - \alpha_0 = \sum_{k=-M-N+1, k\neq 0}^{M+N-1} \alpha_k \left[\frac{\mathbf{x}^* \mathbf{J}_k \mathbf{s}}{\mathbf{x}^* \mathbf{s}}\right] + \frac{\mathbf{x}^* \boldsymbol{\epsilon}}{\mathbf{x}^* \mathbf{s}}. \tag{17}$$

Under the white-noise assumption made in this paper, the variance of the noise-dependent term in (17) is equal to σ^2ISNR, where σ^2 is the noise variance. It follows from this observation and from (17) that, when the values of $\{\alpha_k\}_{k\neq 0}$ and σ^2 are unknown, the minimization of the data-independent metrics introduced above is a natural way of "minimizing" the estimation error in $\hat{\alpha}_0$.

Remark: If information on $\{\alpha_k\}_{k\neq 0}$ and σ^2 were available, for example in the form of previously obtained estimates $\{\hat{\alpha}_k\}_{k\neq 0}$ and $\hat{\sigma}^2$, we would then omit the PSL metric and would combine the ISL and ISNR metrics into a single criterion:

$$\frac{\sum_{k=-M-N+1,k\neq 0}^{M+N-1} |\hat{\alpha}_k|^2 \left|\mathbf{x}^*\mathbf{J}_k\mathbf{s}\right|^2 + \hat{\sigma}^2 \|\mathbf{x}\|^2}{\left|\mathbf{x}^*\mathbf{s}\right|^2}, \tag{18}$$

which should be minimized with respect to the design variables. Note that (18) is an estimate of the variance of $\hat{\alpha}_0$, see (17), under the mild assumption that the returns from different range bins are uncorrelated with one another.

Designs obtained by minimizing (18), or similar criteria, have been considered in the literature, see, e.g., [4], [14], [22]–[24] . We will not consider them in this paper because their computational requirements appear to be well beyond the capabilities of many of the current radar systems. Indeed, while the design obtained by minimizing a data-dependent metric (such as (18)) is not much more complicated to compute than the design derived from a data-independent metric (such as (14) - (16)), the computation of the former has to be done on-line whereas that of the latter can be done off-line (and thus it does not have to meet any hard time constraints). Note that the off-line computation of a data-independent design will produce a code sequence $\{s_n\}$ to be transmitted along with an IV filter vector $\mathbf{x}$ (including its dimension) to be used at the radar receiver, which should be good choices for a whole set of possible scenarios. A data-dependent design, on the other hand, is very much dependent on the assumed scenario and as such it can be rendered completely ineffective by small errors in the assumptions made (such as the errors caused by an unknown Doppler shift that makes the vector multiplying α_0 in (6) be different from the assumed $\mathbf{s}$) [25], [26]. □

Minimum PSL designs have been considered in [16] and [9] - [12]. In the real-valued case, the optimal PSL filter can be obtained by solving a linear program (LP) – see, e.g., [16], [21] and the Appendix A[2]. Alternatively, the minimum-PSL filter can be computed using an iterative algorithm proposed in [11], [12]. The latter algorithm, unlike the LP formulation, can also be used in the complex-valued data case, but its convergence properties are unknown in both cases. In the Appendix A, we explain in passing how to compute the minimum-PSL filter efficiently in both the real-valued case and the complex-valued one.

In this paper, we will focus on the use of the other two metrics in (14) and (16), viz. ISL and ISNR, and therefore we omit any further discussion on the minimum-PSL design. We do so for the sake of conciseness. Additionally, in many cases of practical interest, a well-specified minimum-ISL design can provide more

[2]The original LP formulation in [16] is somewhat different from the LP formulation in [21] and in the Appendix A.

accurate estimates of α_0 than can a minimum-PSL design. This is evidently so in uniformly distributed clutter scenarios. However, this may also be true even in scenarios with a few strong scatterers. Indeed, for the values of M and N often encountered in applications, the sidelobe profile $\{|\mathbf{x}^*\mathbf{J}_k\mathbf{s}|^2 \,/\, |\mathbf{x}^*\mathbf{s}|^2\}$ of a minimum-PSL filter is usually rather flat (see, e.g., [16] for a simple explanation as to why this is so). Therefore, while the PSL of such profile is by definition smaller than the PSL of the corresponding minimum-ISL filter, many sidelobes of the minimum-PSL filter will be higher than the corresponding sidelobes of the minimum-ISL design. The consequence is that the PSL design will give more accurate estimates of α_0 only in the worst-case scenario (that is to say, the case in which the strong scatterers happen to be in the range bins corresponding to the peak sidelobe levels). In the remaining cases, the ISL design is more likely to provide better estimation and detection performance.

Minimum-ISL designs have been considered in [2], [3], [15], [22]–[24] and more recently in [4], [9], [10]. The focus of this tutorial paper is on this type of design, with the main goal to clarify the design problems, highlight the design issues, and point out performance differences among the various possible designs. Compared with most of the previous works, our approach here appears to be both simpler and more complete as well as more logically structured. The principal features of this approach can be summarized as follows:

- The formulation of the design problem involves both ISL and ISNR, as also done in [1], [18].
- An efficient algorithm is presented for solving the joint ISL-ISNR design problem, see also [1], [18].
- Some theoretical properties of the minimum-ISL filter design are reviewed, following [2], [3].
- The design of the code sequence to minimize various performance metrics is also considered, (see, e.g., [5], [7], [8], [22]–[24], [27]–[33] for previous representative works on this aspect).
- Finally, the paper explains how to modify the ISL and ISNR metrics in the case in which the Doppler shift is no longer negligible, and also how to compute the corresponding optimal designs in such a case, similarly to what has been done, for example, in [6], [19], [20], [23], [24], [27], [28], [33], [34].

III. Optimal Designs in the Negligible Doppler Case

We can formulate the design problem either as the minimization of ISL under a constraint on ISNR or as the minimization of ISNR under a constraint on ISL. Here we will concentrate on the second possible formulation because it appears that in practical applications the desired ISL is more easily specified than the desired ISNR (for instance, a value of -50 dB for ISL/$[2(M+N)]$ should be satisfactory for most applications). Nevertheless,

we should stress that the discussion and methods presented in what follows for the second formulation apply with only minor modifications to the aforementioned first formulation as well. Note that below we begin the discussion with an analysis of the problem of minimizing the ISL (without any ISNR constraint), as the results of this analysis are of interest by themselves and they will also turn out to be useful to our study of the design problem of minimizing the ISNR under an upper-bound constraint on ISL.

A. Minimum-ISL Design

The design problem considered in this section consists of minimizing the ISL with respect to $\mathbf{x}$ (for fixed $\mathbf{s}$):

$$\min_{\mathbf{x}} \frac{\sum_{k=-M-N+1,k\neq 0}^{M+N-1} \left|\mathbf{x}^*\mathbf{J}_k\mathbf{s}\right|^2}{\left|\mathbf{x}^*\mathbf{s}\right|^2}. \tag{19}$$

Let

$$\mathbf{R} = \sum_{k=-M-N+1,k\neq 0}^{M+N-1} \mathbf{J}_k\mathbf{s}\mathbf{s}^*\mathbf{J}_k^*. \tag{20}$$

Using this notation, we can rewrite (19) in a more compact form:

$$\min_{\mathbf{x}} \frac{\mathbf{x}^*\mathbf{R}\mathbf{x}}{\left|\mathbf{x}^*\mathbf{s}\right|^2}. \tag{21}$$

The matrix $\mathbf{R}$ can be shown to be strictly positive definite (see Appendix B). Let $\mathbf{R}^{1/2}$ ($\mathbf{R}^{-1/2}$) denote a Hermitian square root of $\mathbf{R}$ (of $\mathbf{R}^{-1}$). Then, by the Cauchy-Schwartz inequality, we have that:

$$\left|\mathbf{x}^*\mathbf{s}\right|^2 = \left|\mathbf{x}^*\mathbf{R}^{1/2}\mathbf{R}^{-1/2}\mathbf{s}\right|^2 \leq (\mathbf{x}^*\mathbf{R}\mathbf{x})(\mathbf{s}^*\mathbf{R}^{-1}\mathbf{s}). \tag{22}$$

This observation implies that:

$$\text{ISL} = \frac{\mathbf{x}^*\mathbf{R}\mathbf{x}}{\left|\mathbf{x}^*\mathbf{s}\right|^2} \geq \frac{1}{\mathbf{s}^*\mathbf{R}^{-1}\mathbf{s}}, \tag{23}$$

where the lower bound is achieved for:

$$\mathbf{x}^{\text{o}} = \mathbf{R}^{-1}\mathbf{s} \quad (\text{or a scaled version thereof}), \tag{24}$$

The minimum value of ISL corresponding to (24) is given by (see (23)):

$$\text{ISL}^{\text{o}} = \frac{1}{\mathbf{s}^*\mathbf{R}^{-1}\mathbf{s}}. \tag{25}$$

Remark: Because the vectors that minimize (21) and the following function:

$$\frac{\sum_{k=-M-N+1}^{M+N-1} \left|\mathbf{x}^*\mathbf{J}_k\mathbf{s}\right|^2}{\left|\mathbf{x}^*\mathbf{s}\right|^2} = \text{ISL} + 1, \tag{26}$$

are identical, we can redefine the matrix $\mathbf{R}$ as

$$\mathbf{R} = \sum_{k=-M-N+1}^{M+N-1} \mathbf{J}_k \mathbf{s}\mathbf{s}^* \mathbf{J}_k^*, \tag{27}$$

and the above results still apply. □

The following important property of the minimum-ISL design was proved in [2], [3] and Appendix C: *ISL^o decreases monotonically as M increases.* Among other things, this property will help us choose the value of M for the design discussed next.

Remark: In lieu of using an IV vector, as in (13), we might think of making use of an IV matrix, let us say $\mathbf{X}$ of dimension $(2M+N) \times \tilde{M}$, where $\tilde{M} \leq 2M+N$. Presumably, the additional degrees of freedom of $\mathbf{X}$ will allow us to obtain improved performance (e.g., a smaller ISL). However, this presumption turns out to be untrue as shown in Appendix D. □

B. Minimum ISNR - Constrained ISL Design

First we specify the values of N and of the desired ISL, which we denote by η. As is well-known, the MF receiver has the smallest ISNR value in the class of IV receivers considered in this paper, namely $\text{ISNR}_{\text{MF}} = 1/\|\mathbf{s}\|^2$, which is equal to $1/N$ for binary sequences. We can choose N so that ISNR_{MF} takes on a reasonably small value; while this value depends on the application, an ISNR_{MF} equal to -10 dB or smaller appears satisfactory for many cases. Note that, whenever the Doppler shifts are not negligible any longer, the choice of N should also take into account the desired accuracy of Doppler estimation, see the next section for details. Regarding η, we can, for instance, choose this parameter such that $\eta/[2(M+N)]$ is around -50 dB (as already mentioned above) – more details on the choice of η will be given shortly.

Next, for the selected value of N and for a "good" code sequence $\{s_n\}$ (for instance the sequence that minimizes the ISL^o in (25)), we compute ISL^o for increasing values of M until we reach a value ISL$^o < \eta$. Depending on the value of η and on the practical constraints on M, we may want to choose an M for which ISL^o is quite a bit smaller than η, if possible (recall that ISL^o decreases continuously as M increases).

Finally, given the values of N, η, and M chosen as outlined above, and for all 2^N possible binary sequences $\{s_n\}$ (assuming that we also want to optimize the code sequence; otherwise $\{s_n\}$ is given by the sequence used to select M), we solve the following constrained minimization problem:

$$\min_{\mathbf{x}} \text{ISNR} \quad \text{s.t.} \quad \text{ISL} \leq \eta. \tag{28}$$

The sequence $\mathbf{s}$ that gives the minimum value of ISNR, let us say $\mathbf{s}^{\circ}$, and the corresponding solution to (28), let us say $\mathbf{x}^{\circ}$, are chosen as the optimal code sequence and optimal IV filter.

To solve (28), we first remind the reader that a scaling of $\mathbf{x}$ does not change either ISNR or ISL. Consequently, there is no restriction to assume that

$$\mathbf{x}^{*}\mathbf{s} = \|\mathbf{s}\|^2 \tag{29}$$

(which is the value of $\mathbf{x}^{*}\mathbf{s}$ corresponding to the MF). Under (29), we can reformulate the IV filter design in (28) as follows:

$$\begin{aligned} \min_{\mathbf{x}} \quad & \|\mathbf{x}\|^2 && (30)\\ \text{s.t.} \quad & \mathbf{x}^{*}\mathbf{s} = \|\mathbf{s}\|^2 && (31)\\ & \mathbf{x}^{*}\mathbf{R}\mathbf{x} \leq \eta\|\mathbf{s}\|^4. && (32) \end{aligned}$$

This is a convex optimization problem that can be efficiently solved by using the Lagrange multiplier methodology (see, e.g., [25]). To make use of the solver presented in the cited paper, we rewrite (30) - (32) as:

$$\begin{aligned} \min_{\mathbf{w}} \quad & \mathbf{w}^{*}\mathbf{R}^{-1}\mathbf{w} && (33)\\ \text{s.t.} \quad & \mathbf{w}^{*}\left(\frac{\mathbf{R}^{-1/2}\mathbf{s}}{\|\mathbf{s}\|^2}\right) = 1 && (34)\\ & \|\mathbf{w}\|^2 \leq \eta\|\mathbf{s}\|^4, && (35) \end{aligned}$$

where $\mathbf{w} = \mathbf{R}^{1/2}\mathbf{x}$. It follows from [25] that the solution to (33) - (35) can be computed as follows. Let

$$\begin{aligned} \mathbf{w}^{\circ}(\lambda) &= \frac{\left(\mathbf{R}^{-1} + \lambda\mathbf{I}\right)^{-1}\mathbf{R}^{-1/2}\mathbf{s}}{\mathbf{s}^{*}\mathbf{R}^{-1/2}\left(\mathbf{R}^{-1} + \lambda\mathbf{I}\right)^{-1}\mathbf{R}^{-1/2}\mathbf{s}}\|\mathbf{s}\|^2 \\ &= \frac{\mathbf{R}^{1/2}\left(\mathbf{I} + \lambda\mathbf{R}\right)^{-1}\mathbf{s}}{\mathbf{s}^{*}\left(\mathbf{I} + \lambda\mathbf{R}\right)^{-1}\mathbf{s}}\|\mathbf{s}\|^2 \triangleq \mathbf{R}^{1/2}\mathbf{x}^{\circ}(\lambda), \end{aligned} \tag{36}$$

where $\lambda > 0$ is a Lagrange multiplier, and

$$\mathbf{x}^{\circ}(\lambda) = \frac{\left(\mathbf{I} + \lambda\mathbf{R}\right)^{-1}\mathbf{s}}{\mathbf{s}^{*}\left(\mathbf{I} + \lambda\mathbf{R}\right)^{-1}\mathbf{s}}\|\mathbf{s}\|^2. \tag{37}$$

First, consider the case in which $\mathbf{w}^{\circ}(0)$ satisfies (see the inequality constraint in (35)):

$$\eta > \frac{\mathbf{s}^{*}\mathbf{R}\mathbf{s}}{\|\mathbf{s}\|^4} \triangleq \eta_{\text{MF}}. \tag{38}$$

Then $\mathbf{w}^{\circ}(0)$ is the solution to (33) - (35), and therefore $\mathbf{x}^{\circ}(0) = \mathbf{s}$ is the solution to (30) - (32). In such a case, the inequality constraint in (35) is inactive.

Next let us assume that (38) does not hold, i.e.,

$$\eta \leq \frac{\mathbf{s}^*\mathbf{R}\mathbf{s}}{\|\mathbf{s}\|^4}. \tag{39}$$

In most applications, this is the case of interest – indeed, the ISL of the MF solution ($\mathbf{x} = \mathbf{s}$), which is evidently equal to η_{MF}, is considered to be too large in many practical situations, and therefore it is quite unlikely that one would choose η as in (38). Now, with reference to (39), η cannot be chosen much smaller than the upper limit in (39) because the problem in (30) - (32) will then become infeasible. To address this concern, we note that the minimum value of $\mathbf{x}^*\mathbf{R}\mathbf{x}/\|\mathbf{s}\|^4$, subject to $\mathbf{x}^*\mathbf{s} = \|\mathbf{s}\|^2$, is equal to $1/(\mathbf{s}^*\mathbf{R}^{-1}\mathbf{s})$. It follows from this observation that the constrained optimization problem in (30) - (32) is feasible if and only if

$$\eta \geq \frac{1}{\mathbf{s}^*\mathbf{R}^{-1}\mathbf{s}} \stackrel{\triangle}{=} \eta_{\text{IV}}. \tag{40}$$

For any value of $\eta \in [\eta_{\text{IV}}, \eta_{\text{MF}}]$ (evidently, $\eta_{\text{IV}} \leq \eta_{\text{MF}}$), it follows from [25] that the solution to (30) - (32) is given by $\mathbf{x}^{\text{o}}(\lambda^{\text{o}})$, where λ^{o} is obtained by solving the secular equation $\|\mathbf{w}^{\text{o}}(\lambda)\|^2 = \eta\|\mathbf{s}\|^4$, or in a more explicit form:

$$\frac{\mathbf{s}^* \left(\mathbf{I} + \lambda\mathbf{R}\right)^{-1} \mathbf{R} \left(\mathbf{I} + \lambda\mathbf{R}\right)^{-1} \mathbf{s}}{\left[\mathbf{s}^* \left(\mathbf{I} + \lambda\mathbf{R}\right)^{-1} \mathbf{s}\right]^2} = \eta. \tag{41}$$

It is also shown in the cited paper that Equation (41) has a unique solution $\lambda^{\text{o}} > 0$, and furthermore that the left-hand side of (41) is a monotonically decreasing function of $\lambda > 0$. Using these observations, the solution of (41) can be efficiently computed.

To conclude this section, we remind the reader that the user's parameter η is pre-specified. Therefore, during the process of combinatorial search for the optimal code sequence, it may happen that the value of η_{IV} associated with some sequences is larger than η. Such sequences can be directly discarded as the constrained optimization problem in (30) - (32) is evidently infeasible for them.

IV. Optimal Designs in the Non-Negligible Doppler Case

When some of the targets illuminated by the radar are moving rapidly with unknown velocities and directions, then their Doppler shifts (assumed to be significant, see below for details) must be taken into account in the data model and the ensuing analysis. Specifically, let $\{\omega_k\}_{k=-M-N+1}^{M+N-1}$ be the Doppler shifts (expressed in radians per second) associated with the range bins under consideration and let

$$\mathbf{s}(\omega) = \left[\begin{array}{ccccc} \mathbf{0}_M^T & s_1 e^{j\omega} & \cdots & s_N e^{jN\omega} & \mathbf{0}_M^T \end{array}\right]^T \tag{42}$$

denote a generic Doppler shifted zero-padded code sequence vector (note that $\mathbf{s}(\omega)$ is complex-valued even when $\mathbf{s}$ is real-valued). Then the data model in (9) should be modified as below whenever the Doppler shifts are not negligible:

$$\mathbf{y} = \alpha_0 \mathbf{s}(\omega_0) + \sum_{k=-M-N+1, k\neq 0}^{M+N-1} \alpha_k \mathbf{J}_k \mathbf{s}(\omega_k) + \boldsymbol{\epsilon}. \tag{43}$$

The ISL and ISNR metrics associated with (43) are given by the following equations:

$$\text{ISL}_{\text{D}} = \sum_{k=-M-N+1, k\neq 0}^{M+N-1} \frac{\left|\mathbf{x}^*(\omega_0)\mathbf{J}_k\mathbf{s}(\omega_k)\right|^2}{\left|\mathbf{x}^*(\omega_0)\mathbf{s}(\omega_0)\right|^2}, \tag{44}$$

and, respectively,

$$\text{ISNR}_{\text{D}} = \frac{\left\|\mathbf{x}(\omega_0)\right\|^2}{\left|\mathbf{x}^*(\omega_0)\mathbf{s}(\omega_0)\right|^2}, \tag{45}$$

where the IV vector depends now on ω_0 (as well as, potentially, on $\{\omega_k\}$; however the dependence on $\{\omega_k\}$ will be eliminated later on, see e.g. (50) below).

Let

$$\Omega = [\omega_a, \omega_b]; \quad \omega_b > \omega_a \tag{46}$$

denote a given interval of possible values of ω_0 and $\{\omega_k\}$ (the set Ω can be obtained as described, e.g., in [4]). Consider the vectors $\mathbf{s}(\omega_a)$ and $\mathbf{s}(\omega_b)$ corresponding to the extreme points of Ω. The submatrix of $\left[\begin{array}{cc} \mathbf{s}(\omega_a) & \mathbf{s}(\omega_b) \end{array}\right]$ that comprises the elements which are different from zero can be written as:

$$\left[\begin{array}{ccc} s_1 & & 0 \\ & \ddots & \\ 0 & & s_N \end{array}\right] \left[\begin{array}{cc} e^{j\omega_a} & e^{j\omega_b} \\ \vdots & \vdots \\ e^{jN\omega_a} & e^{jN\omega_b} \end{array}\right]. \tag{47}$$

It follows from this observation along with well-known properties of the Vandermonde matrices of the form in (47) that the effective rank of the matrix $\left[\begin{array}{cc} \mathbf{s}(\omega_a) & \mathbf{s}(\omega_b) \end{array}\right]$ is two only if the difference $(\omega_b - \omega_a)$ is not much smaller than $2\pi/N$, let us say:

$$(\omega_b - \omega_a) \geq \Delta\omega, \tag{48}$$

where $\Delta\omega$ is on the order of $\pi/(10N)$. This discussion suggests that the Doppler shifts can be considered to be non-negligible whenever the length of the interval Ω, to which they belong, satisfies (48). Let us assume that the following grid

$$\{0, \pm\Delta\omega, \pm 2\Delta\omega, \cdots\} \tag{49}$$

covers Ω; and let L denote the number of points in (49). In a part of the discussion that follows, we will let ω_0 take on the values in the set (49).

Because we do not assume any knowledge about the Doppler shifts $\{\omega_k\}$, other than that they belong to Ω, the ISL metric in (44) cannot be evaluated as it stands. A natural way of circumventing this problem consists of replacing the said metric with the following averaged version of it, over the interval Ω,

$$\text{ISL}_{\text{D}} = \sum_{k=-M-N+1, k\neq 0}^{M+N-1} \left(\frac{1}{\omega_b - \omega_a}\right) \frac{\int_{\Omega} \left|\mathbf{x}^*(\omega_0)\mathbf{J}_k\mathbf{s}(\omega)\right|^2 d\omega}{\left|\mathbf{x}^*(\omega_0)\mathbf{s}(\omega_0)\right|^2}. \tag{50}$$

Remark: Similarly to the comments that we made on (18), we note here that if *a priori* information on the range-Doppler profile were available in a sufficiently precise form, then we could replace (50) by a weighted version that takes into account the expected strengths of the various terms in this equation. The weighted metric can be dealt with in exactly the same manner as the unweighted one in (50) (see below), with only a minor complication of notation. □

Let

$$\mathbf{\Gamma} = \frac{1}{\omega_b - \omega_a} \int_{\Omega} \mathbf{s}(\omega)\mathbf{s}^*(\omega) d\omega. \tag{51}$$

A simple calculation shows that the elements of $\mathbf{\Gamma}$ are either equal to zero or they have the following generic expression:

$$\frac{s_k s_p^*}{(\omega_b - \omega_a)} \int_{\Omega} e^{j(k-p)\omega} d\omega = \begin{cases} |s_k|^2, & \text{for } k = p, \\ \frac{s_k s_p^*}{j(k-p)(\omega_b - \omega_a)} \left[e^{j(k-p)\omega_b} - e^{j(k-p)\omega_a}\right], & \text{for } k \neq p. \end{cases} \tag{52}$$

It follows that:

$$\text{ISL}_{\text{D}} = \frac{\mathbf{x}^*(\omega_0)\mathbf{R}_{\text{D}}\mathbf{x}(\omega_0)}{\left|\mathbf{x}^*(\omega_0)\mathbf{s}(\omega_0)\right|^2}, \tag{53}$$

where

$$\mathbf{R}_{\text{D}} = \sum_{k=-M-N+1, k\neq 0}^{M+N-1} \mathbf{J}_k \mathbf{\Gamma} \mathbf{J}_k^*. \tag{54}$$

For a given ω_0, the ISL and ISNR metrics above have the same form as the corresponding metrics used in the negligible-Doppler case, with the only minor difference that $\mathbf{R}$ in (21) is replaced by $\mathbf{R}_{\text{D}}$ in (53). Consequently, both the *minimum-ISL$_D$ design* and the *minimum ISNR$_D$-constrained ISL$_D$ design* can be efficiently obtained using the methods described in the previous section.

The minimum value of ISL$_{\text{D}}$ with respect to $\mathbf{x}(\omega_0)$, viz.

$$\text{ISL}_{\text{D}}^{\text{o}}(\omega_0) = \frac{1}{\mathbf{s}^*(\omega_0)\mathbf{R}_{\text{D}}^{-1}\mathbf{s}(\omega_0)} \tag{55}$$

decreases with increasing M, as it does in the negligible-Doppler case. This property can be proved as in Appendix C, once we established the fact that the matrices $\mathbf{R}_{\text{D}}$, corresponding to a series of increasing values of M, form a nested sequence (similarly to $\mathbf{R}$). To realize the said fact, observe that $\mathbf{\Gamma}$ can be written as

$$\mathbf{\Gamma} = \sum_{p=1}^{P} \boldsymbol{\gamma}_p \boldsymbol{\gamma}_p^* \tag{56}$$

for some integer P (which can be chosen as the rank of $\mathbf{\Gamma}$) and for some vectors $\{\boldsymbol{\gamma}_p\}$ that have the same zero-padded form as $\mathbf{s}$. Consequently, $\mathbf{R}_{\text{D}}$ can be written as a sum of P matrices, each of which has a similar definition to that of $\mathbf{R}$ in (27). The nested structure of $\mathbf{R}_{\text{D}}$, then, follows from this observation and the nested structure of the matrices of the form of $\mathbf{R}$.

Remark: Note that the larger the Doppler uncertainty interval Ω, the larger is the rank of $\mathbf{\Gamma}$ (see, e.g., [26]). Consequently, the minimum eigenvalue of $\mathbf{R}_{\text{D}}$ may be much larger than that of $\mathbf{R}$, which means that the minimum achievable value of ISL$_{\text{D}}$ may be much larger than that of ISL. Intuitively, this is due to the fact that the designs based on ISL$_{\text{D}}$ are somewhat conservative, as they try to optimize the ISL metric averaged over the entire set Ω; yet there is hardly anything else we could do when the Doppler profile of the scene is completely unknown. □

Next we note that, because ω_0 is not known, we shall compute the desired design for all L values of ω_0 in the set (49). The so-obtained IV filter vectors $\mathbf{x}(\omega_0)$ or quantities related to them (see below), for $\omega_0 = 0, \pm\Delta\omega, \pm 2\Delta\omega, \cdots$, which can be pre-computed, will be used at the receiver to estimate both α_0 and ω_0. Specifically, α_0 is estimated using basically the same formula as in the previous section (see (13)):

$$\hat{\alpha}_0 = \frac{\mathbf{x}^*(\hat{\omega}_0)\mathbf{y}}{\mathbf{x}^*(\hat{\omega}_0)\mathbf{s}(\hat{\omega}_0)} = \frac{\mathbf{s}^*(\hat{\omega}_0)\tilde{\mathbf{R}}_{\text{D}}^{-1}\mathbf{y}}{\mathbf{s}^*(\hat{\omega}_0)\tilde{\mathbf{R}}_{\text{D}}^{-1}\mathbf{s}(\hat{\omega}_0)}, \tag{57}$$

where $\tilde{\mathbf{R}}_{\text{D}} = \mathbf{R}_{\text{D}}$ for the minimum-ISL$_{\text{D}}$ design, and $\tilde{\mathbf{R}}_{\text{D}} = \mathbf{I} + \lambda\mathbf{R}_{\text{D}}$ for the minimum ISNR$_{\text{D}}$-constrained ISL$_{\text{D}}$ design. Furthermore, the estimate $\hat{\omega}_0$ of ω_0 in (57) is given by the solution to the following maximization problem:

$$\max_{\omega_0 \in \{0, \pm\Delta\omega, \pm 2\Delta\omega, \cdots\}} \frac{\left|\mathbf{s}^*(\omega_0)\tilde{\mathbf{R}}_{\text{D}}^{-1}\mathbf{y}\right|^2}{\mathbf{s}^*(\omega_0)\tilde{\mathbf{R}}_{\text{D}}^{-1}\mathbf{s}(\omega_0)}. \tag{58}$$

To motivate (58), note that $\tilde{\mathbf{R}}_{\text{D}}$ can be interpreted as a guess of a scaled version of the covariance matrix of the clutter and noise in the minimum ISNR_{D}-constrained ISL_{D} design case, or only of the clutter covariance matrix in the minimum-ISL_{D} design case (note also that in the case of the former design, $\tilde{\mathbf{R}}_{\text{D}}$ may depend on ω_0 via $\lambda(\omega_0)$; however, the dependence of $\lambda(\omega_0)$ on ω_0 is expected to be fairly weak in general and is therefore omitted in what follows). With this fact in mind, consider the following weighted least-squares fitting criterion:

$$\left\| \tilde{\mathbf{R}}_{\text{D}}^{-1/2} \left[\mathbf{y} - \alpha_0 \mathbf{s}(\omega_0) \right] \right\|^2. \tag{59}$$

The minimization of (59) with respect to α_0, for fixed ω_0, evidently gives the optimal IV estimate in (57). Insertion of (57) (with $\hat{\omega}_0$ replaced by ω_0) into (59) yields the function:

$$\begin{aligned} & \left\| \tilde{\mathbf{R}}_{\text{D}}^{-1/2} \mathbf{y} - \frac{\tilde{\mathbf{R}}_{\text{D}}^{-1/2} \mathbf{s}(\omega_0) \mathbf{s}^*(\omega_0) \tilde{\mathbf{R}}_{\text{D}}^{-1} \mathbf{y}}{\mathbf{s}^*(\omega_0) \tilde{\mathbf{R}}_{\text{D}}^{-1} \mathbf{s}(\omega_0)} \right\|^2 \\ = & \left\| \left[\mathbf{I} - \frac{\tilde{\mathbf{R}}_{\text{D}}^{-1/2} \mathbf{s}(\omega_0) \mathbf{s}^*(\omega_0) \tilde{\mathbf{R}}_{\text{D}}^{-1/2}}{\mathbf{s}^*(\omega_0) \tilde{\mathbf{R}}_{\text{D}}^{-1} \mathbf{s}(\omega_0)} \right] \tilde{\mathbf{R}}_{\text{D}}^{-1/2} \mathbf{y} \right\|^2 \\ = & \mathbf{y}^* \tilde{\mathbf{R}}_{\text{D}}^{-1/2} \left[\mathbf{I} - \frac{\tilde{\mathbf{R}}_{\text{D}}^{-1/2} \mathbf{s}(\omega_0) \mathbf{s}^*(\omega_0) \tilde{\mathbf{R}}_{\text{D}}^{-1/2}}{\mathbf{s}^*(\omega_0) \tilde{\mathbf{R}}_{\text{D}}^{-1} \mathbf{s}(\omega_0)} \right] \tilde{\mathbf{R}}_{\text{D}}^{-1/2} \mathbf{y}. \end{aligned} \tag{60}$$

The estimate $\hat{\omega}_0$ of the Doppler shift for the range bin of current interest is obtained by minimizing (60) with respect to ω_0, or equivalently by solving the maximization problem in (58).

V. Numerical Case Studies and Concluding Remarks

We discuss first a negligible-Doppler case and then a case in which the Doppler shift can no longer be neglected. In the numerical studies of this section we focus on the use of binary sequences $\{s_n\}_{n=1}^N$.

A. Negligible-Doppler Case

We consider the MF design and the following two *minimum-ISL designs* (for given values of N and M):

- $\mathbf{x}_1 = \mathbf{s}_1$, where $\mathbf{s}_1$ is the zero-padded binary sequence that minimizes

$$\text{the ISL of MF:} \quad \mathbf{s}_1 = \arg\min_{\mathbf{s}} \mathbf{s}^* \mathbf{R} \mathbf{s}, \tag{61}$$

- $\mathbf{x}_2 = \mathbf{R}^{-1} \mathbf{s}_1$, (62)

- $\mathbf{x}_3 = \mathbf{R}^{-1} \mathbf{s}_2$, where $\mathbf{s}_2$ is the zero-padded binary sequence that minimizes

$$\text{the ISL of IV:} \quad \mathbf{s}_2 = \arg\max_{\mathbf{s}} \mathbf{s}^* \mathbf{R}^{-1} \mathbf{s}. \tag{63}$$

We also consider two *minimum ISNR-constrained ISL designs* (once again, for given values of N and M):

- $\mathbf{x}_4 =$ the solution to the design problem in (28) for $\mathbf{s} = \mathbf{s}_2$
  and $\eta = \text{ISL}(\mathbf{x}_3) + 35$ dB for $N = 16$ and $\eta = \text{ISL}(\mathbf{x}_3) + 25$ dB for $N = 21$, (64)
- $\mathbf{x}_5 =$ defined similarly to $\mathbf{x}_4$, but with $\mathbf{s}$ equal to the zero-padded binary sequence
  that gives the smallest value of ISNR among all vectors of $\mathbf{s}$ for which $\mathbf{x}_4$ exists. (65)

The ISL, PSL, and ISNR metrics, as functions of M, corresponding to the above five designs are shown in Figure 1 for both $N = 16$ and $N = 21$. The results presented in the figure allow us to make a number of relevant observations on the behavior of the designs under consideration:

(i) As M increases, the ISL and PSL metrics associated with the IV designs $\mathbf{x}_2$ and $\mathbf{x}_3$ take on much smaller values than the values corresponding to the MF design $\mathbf{x}_1$, at the cost of a relatively minor loss in ISNR. As an example, ISL($\mathbf{x}_3$) for $N = 16$ and $M = 80$ is smaller than ISL($\mathbf{x}_1$) by some 100 dB, whereas the ISNR loss of $\mathbf{x}_3$ compared with $\mathbf{x}_1$ is only 1.70 dB.

(ii) The ISL and PSL performance of $\mathbf{x}_3$ is much better than that of $\mathbf{x}_2$, which shows the importance of designing the probing sequence $\{\mathbf{s}_n\}$ in addition to designing the receive filter $\mathbf{x}$; indeed, for example, at $N = 16$ and $M = 80$, the ISL of $\mathbf{x}_3$ is smaller than the ISL of $\mathbf{x}_2$ by 66.36 dB. The ISNR of $\mathbf{x}_3$ is larger than that of $\mathbf{x}_2$ by approximately 1.15 dB for $N = 21$; but for $N = 16$ the ISNR of $\mathbf{x}_3$ is smaller than the ISNR of $\mathbf{x}_2$ for $M \geq 40$ – consequently, in the case of $N = 16$ and for $M \geq 40$, $\mathbf{x}_3$ outperforms $\mathbf{x}_2$ with respect to all three metrics (ISL, PSL, and ISNR).

The sequence $\mathbf{s}_2$ employed by $\mathbf{x}_3$ evidently changes as N changes, but it can also vary with M. The sequences $\mathbf{s}_2$ for $N = 16$ and $N = 21$, and for $M = 0$, 20, 40, 60 and 80 are given in Table I (omitting the zero-padded segments). Note that the solution to the design problem that leads to $\mathbf{s}_2$ is not necessarily unique, which explains why several sequences $\mathbf{s}_2$ occur in Table I for some pairs (N, M).

(iii) The differences in the ISL and PSL performances of $\mathbf{x}_1$, $\mathbf{x}_2$, and $\mathbf{x}_3$, for a given value of M, decrease as N increases. In fact the said differences appear to depend mainly on the ratio M/N – the larger this ratio, the larger the differences between the performances of the three designs. To illustrate this dependence of ISL (and PSL) on the ratio M/N, we note that the ISL of $\mathbf{x}_2$ with $\mathbf{s}$ equal to a zero-padded extended Legendre sequence [35] of length $N = 300$ is equal to about -40 dB at $M = 1500$,

therefore for $M/N = 5$; and that a similar ISL value around -40 dB is attained by $\mathbf{x}_2$ for $N = 16$ and $M = 80$ (see Figure 1), therefore also for $M/N = 5$.

The main implication of the above observation is that in general we should choose a "small" value for N rather than a "large" one. Of course, the smallest value of N that we can choose is dictated by the desired ISNR. If we will significantly increase N beyond that value, then we will decrease the ISNR, but the values of ISL and PSL might become too large for any practically feasible value of M, and the computation of the designs $\mathbf{x}_3$ and $\mathbf{x}_5$ (which are based on optimizing the probing sequence) may well become intractable.

(iv) The designs $\mathbf{x}_4$ and $\mathbf{x}_5$ have been computed only for $M \geq 60$ because their associated ISL (which is equal to ISL$(\mathbf{x}_3) + 35$ dB for $N = 16$ and to ISL$(\mathbf{x}_3) + 25$ dB for $N = 21$, as explained above) was considered to be "too large" for smaller values of M (see Figure 1). In the case of $N = 16$, the difference between these two designs is relatively small for all three metrics (note that $\mathbf{x}_4$ and $\mathbf{x}_5$ have the same ISL values, by design). For the said value of N, the imposed ISL loss of 35 dB, compared with $\mathbf{x}_3$, results in an ISNR gain of 0.65 dB for $\mathbf{x}_5$– hence reducing the ISNR loss compared with MF to 1.03 dB. For $N = 21$, on the other hand, $\mathbf{x}_5$ has a significantly smaller ISNR than $\mathbf{x}_4$ – indeed, in this case the ISNR gain of $\mathbf{x}_5$ over $\mathbf{x}_4$ is approximately 1.30 dB. Interestingly, we have here another instance of a design that can outperform another one in terms of all three metrics (see also the discussion in point (ii) above): in effect $\mathbf{x}_5$ is better than $\mathbf{x}_2$ with respect to both ISL and PSL as well as ISNR.

The sequences $\mathbf{s}_3$ used in $\mathbf{x}_5$, for $N = 16$ and $N = 21$ and for $M = 60$ and $M = 80$, are presented in Table II (omitting the zero-padded segments).

The above remarks and observations suggest the following *recommendations*. In a scenario in which the ISL and PSL are the key features, ISNR being less important, we can think of using $\mathbf{x}_3$ with a relatively small value of N and with an M several times larger than N. On the other hand, if ISNR is deemed to be an important feature, we can use $\mathbf{x}_5$ to tradeoff an ISL and PSL loss for an ISNR gain, possibly with a larger value of N than that recommendable for the previous scenario.

B. Non-Negligible Doppler Case

Let

$$\Delta\omega = \Phi\left(\frac{\pi}{180^\circ}\right)\left(\frac{1}{N}\right) \tag{66}$$

and consider the Doppler shift set in (46) with $\omega_a = -\Delta\omega$ and $\omega_b = \Delta\omega$, i.e.,

$$\Omega = [-\Delta\omega, \Delta\omega]\,. \tag{67}$$

It follows from (66) and (67) that Φ is the maximum considered Doppler shift (in degrees) over the length of the code sequence. In most of the examples that follow we will let $\Phi = 5^\circ$. This value is analogous to the Doppler shift of a target with an approximate velocity of Mach 2 illuminated by a 1 μs pulse from an S-band radar (see, e.g., [36]).

We consider the following *minimum-ISL$_{\text{D}}$ designs*, in addition to the MF design:

- $\mathbf{x}_1(\omega_0) = \mathbf{s}_1(\omega_0)$, where $\mathbf{s}_1$ is given by (61), (68)
- $\mathbf{x}_6(\omega_0) = \mathbf{R}_{\text{D}}^{-1}\mathbf{s}_1(\omega_0)$, (69)
- $\mathbf{x}_7(\omega_0) = \mathbf{R}_{\text{D}}^{-1}\mathbf{s}_4(\omega_0)$, where $\mathbf{s}_4$ is the zero-padded binary sequence that gives the smallest value of $\text{ISL}_{\text{D}}^{\circ}(\omega_0)$ averaged over the set $\{0, \pm\Delta\omega\}$, i.e.

$$\sum_{\omega_0\in\{0,\pm\Delta\omega\}} \text{ISL}_{\text{D}}^{\circ}(\omega_0). \tag{70}$$

We also consider the following two *minimum ISNR$_{\text{D}}$-constrained ISL$_{\text{D}}$ designs*:

- $\mathbf{x}_8(\omega_0) =$ the solution to the minimum ISNR_{D}-constrained ISL_{D} problem with $\mathbf{s} = \mathbf{s}_4$ (the sequence used by $\mathbf{x}_7(\omega_0)$) and $\eta = \text{ISL}_{\text{D}}(\mathbf{x}_6(\omega_0))$, (71)
- $\mathbf{x}_9(\omega_0) =$ defined similarly to $\mathbf{x}_8(\omega_0)$ but with $\mathbf{s} = \mathbf{s}_5$ – the zero-padded binary sequence that gives the smallest value of $\text{ISNR}_{\text{D}}(\omega_0)$ averaged over the set $\{0, \pm\Delta\omega\}$, or equivalently, the smallest value of the following averaged norm:

$$\sum_{\omega_0\in\{0,\pm\Delta\omega\}} ||\mathbf{x}_8(\omega_0)||^2. \tag{72}$$

Several performance metrics (see below for details), associated with the above designs, have been computed for $\omega_0 = 0$, $\omega_0 = \Delta\omega$ and $\omega_0 = -\Delta\omega$. For all designs, the performance metrics have been observed to be quite insensitive to the value taken by ω_0. This was somewhat expected: as mentioned in the remark that follows

Equation (56), the performance of the considered designs is expected to degrade quite a bit as the size of the uncertainty Doppler shift set increases, but the dependence on ω_0 will typically be much weaker. With this fact in mind, and also in an attempt to keep the number of plots included under control, we will show the results obtained only for $\omega_0 = 0$ (the results corresponding to $\omega_0 = \Delta\omega$ and $\omega_0 = -\Delta\omega$ were almost indistinguishable from those for $\omega_0 = 0$, in most cases).

Figures 2 and 3 show the ISL_{D} and ISNR_{D} metrics, respectively, associated with the designs $\mathbf{x}_1$, $\mathbf{x}_6$, $\mathbf{x}_7$, $\mathbf{x}_8$ and $\mathbf{x}_9$, as functions of M, for $\Phi = 1^\circ$, 5°, 10° and 15°, and for both $N = 16$ and $N = 21$.

Tables III and IV give the optimal sequences $\mathbf{s}_4$ and $\mathbf{s}_5$, used by $\mathbf{x}_7/\mathbf{x}_8$ and $\mathbf{x}_9$, for several values of M and for $\Phi = 5^\circ$.

For the next numerical illustrations we set $M = 60$ and $\Phi = 5^\circ$. Figure 4 shows the sidelobe profiles

$$\text{SL}(k,\omega) = \frac{\left|\mathbf{x}^*(\omega_0)\mathbf{J}_k\mathbf{s}(\omega)\right|^2}{\left|\mathbf{x}^*(\omega_0)\mathbf{s}(\omega_0)\right|^2} \tag{73}$$

as functions of k and ω (the so-called cross-ambiguity functions), associated with the designs under consideration, for both $N = 16$ and $N = 21$.

We also show in Figure 5 the corresponding ISL and PSL metrics, as functions of ω, namely

$$\text{ISL}(\omega) = \sum_{k=-M-N+1, k\neq 0}^{M+N-1} \text{SL}(k,\omega), \tag{74}$$

and

$$\text{PSL}(\omega) = \max_{k\neq 0} \text{SL}(k,\omega). \tag{75}$$

The following observations can be made based on the results shown in the figures:

(i) Much as in the negligible-Doppler case, the ISL_{D} gains of $\mathbf{x}_6$ and especially of $\mathbf{x}_7$ over $\mathbf{x}_1$ become significant as M increases, at the cost of a relatively minor ISNR_{D} loss for $N = 16$ and a mild one for $N = 21$. The design $\mathbf{x}_9$ can be used to eliminate part of the said ISNR_{D} loss, and still achieve the same ISL_{D} as $\mathbf{x}_6$.

(ii) While the ISNR_{D} values in the figures are in most cases similar to those encountered in the negligible-Doppler case (with the exception of $\mathbf{x}_7$ for which the ISNR_{D} values are larger than the corresponding ISNR ones), the ISL_{D} values associated with the IV designs are much larger. Moreover, the larger the value of Φ, the faster the convergence of ISL_{D} to a constant as M increases. An implication of the

latter fact is that in the non-negligible-Doppler case we should choose a (much) smaller value of M than in the negligible-Doppler case.

(iii) We can see from Figures 4 and 5 that, as expected, the ISL and PSL performances of the designs degrade as the magnitude of the Doppler shift takes on larger values. This degradation is more significant for the design $\mathbf{x}_7$ than for the other designs for which the performance degrades quite gracefully. Despite the said performance degradation, the IV designs still offer much better performance than that of the MF design, for the range of Doppler shifts considered here.

(iv) The designs $\mathbf{x}_7$ and $\mathbf{x}_9$, which use optimal sequences $\{\mathbf{s}_n\}$, perform better than the corresponding designs $\mathbf{x}_6$ and $\mathbf{x}_8$, respectively, which use non-optimal sequences.

Similarly to the conclusion presented at the end of the previous sub-section, we therefore *recommend* the use of $\mathbf{x}_7$ or $\mathbf{x}_9$, depending on whether the ISL or the ISNR (respectively) is the metric of most interest. The design $\mathbf{x}_6$ was also found to be quite competitive in our numerical studies, and it may be the recommended design particularly in those cases in which the chosen value of N is too large for the computation of $\mathbf{x}_7$ or $\mathbf{x}_9$ to be feasible.

APPENDIX A. COMPUTATION OF THE MINIMUM-PSL FILTER

Following the approach of [21], we write the vector $\mathbf{x}$ as:

$$\mathbf{x} = \mathbf{s} + \mathbf{U}\mathbf{z}, \tag{76}$$

where the $(2M+N)\times(2M+N-1)$ matrix $\mathbf{U}$ comprises a unitary basis of the null space of $\mathbf{s}^*$, that is to say $\mathbf{U}^*\mathbf{s}=\mathbf{0}$ and $\mathbf{U}^*\mathbf{U}=\mathbf{I}$ (note that the PSL metric, similar to the ISL and ISNR metrics, is invariant to the scaling of $\mathbf{x}$ and therefore we can choose the coefficient multiplying $\mathbf{s}$ in the decomposition in (76) to be 1). Using (76) in Equation (15) for PSL we get the following cost function:

$$\frac{\left|\mathbf{s}^*\mathbf{J}_k\mathbf{s}+\mathbf{z}^*\mathbf{U}^*\mathbf{J}_k\mathbf{s}\right|^2}{\|\mathbf{s}\|^4}. \tag{77}$$

Consequently the minimum-PSL filter vector is given by the solution to the problem:

$$\min_{\mathbf{x},\gamma} \quad \gamma \tag{78}$$

$$\text{s.t.} \quad \left|\mathbf{s}^*\mathbf{J}_k^*\mathbf{s}+\mathbf{s}^*\mathbf{J}_k^*\mathbf{U}\mathbf{z}\right|^2 \le \gamma\|\mathbf{s}\|^4, \tag{79}$$

$$\text{for } k=-M-N+1,\cdots,-1,1,\cdots,M+N-1,$$

where γ is an auxiliary variable.

In the real-valued case, the problem above is a simple linear program (LP). In the complex-valued case, the above problem is a second-order cone program (SOCP) [37] that can be efficiently solved in polynomial time by means of public-domain software (see, e.g., [38], [39]). The SOCP solver has guaranteed convergence, unlike the iterative solution method proposed in [11] whose convergence properties appear to be unknown.

Remark: The additive decomposition in (76) also allows us to provide a simple explanation of the fact that the use of a code sequence $\mathbf{s}$ with good PSL or ISL properties leads to a PSL- or ISL-optimal IV filter whose ISNR is only slightly larger than that of the MF. (This fact has been amply illustrated numerically in the literature, see, e.g., [9], [10], but never quite explained directly). Indeed, the said decomposition shows that whenever $\mathbf{s}$ has good PSL/ISL properties, then $\mathbf{z}$ in the "correction term" in (76) is likely to have a small norm; this observation, when combined with the fact that

$$\text{ISNR}_{\text{IV}} = \frac{\|\mathbf{s}\|^2 + \|\mathbf{z}\|^2}{\|\mathbf{s}\|^4} = \text{ISNR}_{\text{MF}} \left(1 + \frac{\|\mathbf{z}\|^2}{\|\mathbf{s}\|^2} \right), \tag{80}$$

provides the desired explanation. □

APPENDIX B. PROOF THAT THE MATRIX $\mathbf{R}$ IS POSITIVE DEFINITE

Let $\mathbf{C}$ be the following $(2M+N) \times (2M+N)$ matrix:

$$\mathbf{C} = \begin{bmatrix} \mathbf{C}_1 & \mathbf{0} \\ \mathbf{0} & \mathbf{C}_2 \end{bmatrix}, \tag{81}$$

where the $(M+1) \times (M+1)$ matrix $\mathbf{C}_1$ is given by

$$\mathbf{C}_1 = \begin{bmatrix} s_N & \cdots & \\ & \ddots & \vdots \\ 0 & & s_N \end{bmatrix}, \tag{82}$$

and the $(M+N-1) \times (M+N-1)$ matrix $\mathbf{C}_2$ is defined as

$$\mathbf{C}_2 = \begin{bmatrix} s_1 & & 0 \\ \vdots & \ddots & \\ & \cdots & s_1 \end{bmatrix}. \tag{83}$$

Because $s_1 s_N \neq 0$ (otherwise, the length of the probing sequence $\{s_n\}_{n=1}^N$ is less than the assumed value of N), it follows that $\det(\mathbf{C}) \neq 0$, where $\det(\cdot)$ denotes the determinant of a matrix. This fact implies that the matrix $\mathbf{R}$, which can be written in the form:

$$\mathbf{R} = \left[\begin{array}{cc} \mathbf{C} & \tilde{\mathbf{C}} \end{array} \right] \left[\begin{array}{c} \mathbf{C}^* \\ \tilde{\mathbf{C}}^* \end{array} \right] = \mathbf{C}\mathbf{C}^* + \tilde{\mathbf{C}}\tilde{\mathbf{C}}^*, \tag{84}$$

for some matrix $\tilde{\mathbf{C}}$ (whose exact expression is not of interest to this proof), must be strictly positive definite.

APPENDIX C. PROOF THAT ISL^o DECREASES AS M INCREASES

We will attach an index M to $\mathbf{s}$, $\mathbf{x}$ and $\mathbf{R}$ to indicate their dependence on this parameter. Clearly, $\mathbf{s}_{M+1}$ has the following nested structure:

$$\mathbf{s}_{M+1} = \left[\begin{array}{c} \mathbf{0} \\ \mathbf{s}_M \\ \mathbf{0} \end{array} \right]. \tag{85}$$

In view of (85), we can also write $\mathbf{x}_{M+1}$ in the following nested form:

$$\mathbf{x}_{M+1} = \left[\begin{array}{c} \rho \\ \mathbf{x}_M \\ \tilde{\rho} \end{array} \right], \tag{86}$$

where ρ and $\tilde{\rho}$ are scalar variables. Furthermore, it is straightforward to verify that

$$\mathbf{x}_M^* \mathbf{s}_M = \mathbf{x}_{M+1}^* \mathbf{s}_{M+1}, \tag{87}$$

and that

$$\begin{aligned} \mathbf{x}_M^* \mathbf{R}_M \mathbf{x}_M &= \mathbf{x}_M^* \left[\begin{array}{ccc} \mathbf{0}_{2M+N} & \mathbf{I}_{2M+N} & \mathbf{0}_{2M+N} \end{array} \right] \mathbf{R}_{M+1} \left[\begin{array}{c} \mathbf{0}_{2M+N}^T \\ \mathbf{I}_{2M+N} \\ \mathbf{0}_{2M+N}^T \end{array} \right] \mathbf{x}_M, \\ &= \left(\mathbf{x}_{M+1}^* \mathbf{R}_{M+1} \mathbf{x}_{M+1} \right) \Big|_{\rho=\tilde{\rho}=0}, \end{aligned} \tag{88}$$

where $\mathbf{0}_M$ denotes the $M \times 1$ all-zero vector and $\mathbf{I}_M$ denotes the identity matrix of dimension M. It follows from (87) and (88) that:

$$\frac{\mathbf{x}_M^* \mathbf{R}_M \mathbf{x}_M}{\left| \mathbf{x}_M^* \mathbf{s}_M \right|^2} = \left. \frac{\mathbf{x}_{M+1}^* \mathbf{R}_{M+1} \mathbf{x}_{M+1}}{\left| \mathbf{x}_{M+1}^* \mathbf{s}_{M+1} \right|^2} \right|_{\rho=\tilde{\rho}=0}, \tag{89}$$

which implies immediately that $\text{ISL}^{\text{o}}_{M+1} \leq \text{ISL}^{\text{o}}_{M}$ (because the optimal values of ρ and $\tilde{\rho}$ cannot produce a larger value of ISL than $\rho = \tilde{\rho} = 0$).

A more quantitative analysis of the difference $\text{ISL}^{\text{o}}_{M} - \text{ISL}^{\text{o}}_{M+1}$ runs as follows. Let $\mathbf{V}$ denote the matrix post-multiplying $\mathbf{R}_{M+1}$ in (88), viz.

$$\mathbf{V} = \begin{bmatrix} \mathbf{0}^T_{2M+N} \\ \mathbf{I}_{2M+N} \\ \mathbf{0}^T_{2M+N} \end{bmatrix}. \tag{90}$$

Then:

$$\begin{aligned} \frac{1}{\text{ISL}^{\text{o}}_{M+1}} - \frac{1}{\text{ISL}^{\text{o}}_{M}} &= \mathbf{s}^*_{M+1}\mathbf{R}^{-1}_{M+1}\mathbf{s}_{M+1} - \mathbf{s}^*_{M+1}\mathbf{V}\left(\mathbf{V}^*\mathbf{R}_{M+1}\mathbf{V}\right)^{-1}\mathbf{V}^*\mathbf{s}_{M+1} \\ &= \mathbf{s}^*_{M+1}\mathbf{R}^{-1/2}_{M+1}\left[\mathbf{I} - \mathbf{R}^{1/2}_{M+1}\mathbf{V}\left(\mathbf{V}^*\mathbf{R}_{M+1}\mathbf{V}\right)^{-1}\mathbf{V}^*\mathbf{R}^{1/2}_{M+1}\right]\mathbf{R}^{-1/2}_{M+1}\mathbf{s}_{M+1} \\ &\stackrel{\triangle}{=} \mathbf{s}^*_{M+1}\mathbf{R}^{-1/2}_{M+1}\mathbf{P}^{\perp}_{\mathbf{R}^{1/2}_{M+1}\mathbf{V}}\mathbf{R}^{-1/2}_{M+1}\mathbf{s}_{M+1}, \end{aligned} \tag{91}$$

where $\mathbf{P}^{\perp}_{\mathbf{R}^{1/2}_{M+1}\mathbf{V}}$ denotes the orthogonal projection matrix onto the null space of $\left(\mathbf{R}^{1/2}_{M+1}\mathbf{V}\right)^*$. Because $\mathbf{P}^{\perp}_{\mathbf{R}^{1/2}_{M+1}\mathbf{V}}$ is a positive semi-definite matrix, it follows from (91) that $\text{ISL}^{\text{o}}_{M+1} \leq \text{ISL}^{\text{o}}_{M}$ (as also proved before). Furthermore, (91) shows that the equality $\text{ISL}^{\text{o}}_{M+1} = \text{ISL}^{\text{o}}_{M}$ holds if and only if there is an $(2M+N)$-vector $\boldsymbol{\beta}$ such that $\mathbf{R}^{-1/2}_{M+1}\mathbf{s}_{M+1} = \mathbf{R}^{1/2}_{M+1}\mathbf{V}\boldsymbol{\beta}$, or equivalently:

$$\mathbf{s}_{M+1} = \mathbf{R}_{M+1}\mathbf{V}\boldsymbol{\beta}. \tag{92}$$

Because the condition above appears hard to satisfy, we conclude that in general $\text{ISL}^{\text{o}}_{M+1}$ is strictly smaller than $\text{ISL}^{\text{o}}_{M}$.

APPENDIX D: IV MATRIX FILTERS ARE NOT BETTER THAN IV VECTOR FILTERS

Let $\mathbf{X}$ be the $(2M+N) \times \tilde{M}$ matrix mentioned in the Remark at the end of Section III-A. Pre-multiplication of (9) with $\mathbf{X}^*$ yields the equation:

$$\mathbf{X}^*\mathbf{y} = \alpha_0\mathbf{X}^*\mathbf{s} + \sum_{k=-M-N+1, k\neq 0}^{M+N-1} \alpha_k\mathbf{X}^*\mathbf{J}_k\mathbf{s} + \mathbf{X}^*\boldsymbol{\epsilon}. \tag{93}$$

The LS estimate of α_0 in the above equation is given by

$$\begin{aligned} \hat{\alpha}_0 &= \frac{\mathbf{s}^*\mathbf{X}\mathbf{X}^*\mathbf{y}}{\|\mathbf{X}^*\mathbf{s}\|^2} \\ &= \alpha_0 + \sum_{k=-M-N+1, k\neq 0}^{M+N-1} \alpha_k \frac{\mathbf{s}^*\mathbf{X}\mathbf{X}^*\mathbf{J}_k\mathbf{s}}{\|\mathbf{X}^*\mathbf{s}\|^2} + \frac{\mathbf{s}^*\mathbf{X}\mathbf{X}^*\boldsymbol{\epsilon}}{\|\mathbf{X}^*\mathbf{s}\|^2}. \end{aligned} \tag{94}$$

It follows from (94) that in the present case, the ISL and ISNR metrics should be defined as follows (the PSL metric can be defined similarly, but we do not consider it in this appendix for brevity's sake):

$$\text{ISL} = \sum_{k=-M-N+1, k\neq 0}^{M+N-1} \frac{\left|\mathbf{s}^*\mathbf{X}\mathbf{X}^*\mathbf{J}_k\mathbf{s}\right|^2}{\left\|\mathbf{X}^*\mathbf{s}\right\|^4} = \frac{\mathbf{s}^*\mathbf{X}\mathbf{X}^*\mathbf{R}\mathbf{X}\mathbf{X}^*\mathbf{s}}{\left(\mathbf{s}^*\mathbf{X}\mathbf{X}^*\mathbf{s}\right)^2}, \tag{95}$$

where $\mathbf{R}$ is as defined in (20), and

$$\text{ISNR} = \frac{\mathbf{s}^*\mathbf{X}\mathbf{X}^*\mathbf{X}\mathbf{X}^*\mathbf{s}}{\left(\mathbf{s}^*\mathbf{X}\mathbf{X}^*\mathbf{s}\right)^2}. \tag{96}$$

Observe that the ISNR metric can be interpreted as a special case of the ISL metric corresponding to $\mathbf{R} = \mathbf{I}$. With this fact in mind, in the following we focus on the ISL metric. We will show that *the value of this metric associated with any IV matrix* $\mathbf{X}$ *can also be achieved with an IV vector* $\mathbf{x}$ (related to $\mathbf{X}$ in a way that will be detailed below).

The expression for the ISL in (95), corresponding to the matrix case, appears to be much more complicated than the vector case expression in (21). However, (95) can be simplified by using an additive decomposition of $\mathbf{X}$, which is the extension of the decomposition in (76) to the matrix case, namely:

$$\mathbf{X} = \mathbf{P}_\mathbf{s}\mathbf{X} + \mathbf{P}_\mathbf{s}^\perp\mathbf{X}, \tag{97}$$

where

$$\mathbf{P}_\mathbf{s} = \frac{\mathbf{s}\mathbf{s}^*}{\left\|\mathbf{s}\right\|^2}, \tag{98}$$

$$\mathbf{P}_\mathbf{s}^\perp = \mathbf{I} - \mathbf{P}_\mathbf{s} = \mathbf{U}\mathbf{U}^*; \quad \mathbf{U}^*\mathbf{U} = \mathbf{I}, \tag{99}$$

and where $\mathbf{U}$ comprises a unitary basis of the null space of $\mathbf{s}^*$ (like in (76)). Using (98) and (99) in (97), we can write $\mathbf{X}$ as:

$$\mathbf{X} = \mathbf{s}\mathbf{w}^* + \mathbf{U}\mathbf{Z}, \tag{100}$$

for some $\tilde{M} \times 1$ vector $\mathbf{w}$ and some $(2M+N-1) \times \tilde{M}$ matrix $\mathbf{Z}$ whose exact expressions are not important for this proof. Because multiplication of $\mathbf{X}$ by any non-zero constant does not change the ISL, we can assume without introducing any restriction that $\left\|\mathbf{w}\right\|^2 = 1$. A simple calculation based on (100) then shows that:

$$\mathbf{s}^*\mathbf{X}\mathbf{X}^*\mathbf{s} = \left\|\mathbf{s}\right\|^4, \tag{101}$$

and

$$\begin{aligned} \mathbf{s}^*\mathbf{X}\mathbf{X}^*\mathbf{R}\mathbf{X}\mathbf{X}^*\mathbf{s} &= \left\|\mathbf{s}\right\|^4 \mathbf{w}^* \left(\mathbf{w}\mathbf{s}^* + \mathbf{Z}^*\mathbf{U}^*\right) \mathbf{R} \left(\mathbf{s}\mathbf{w}^* + \mathbf{U}\mathbf{Z}\right) \mathbf{w} \\ &= \left\|\mathbf{s}\right\|^4 \left\|\mathbf{R}^{1/2}\left(\mathbf{s} + \mathbf{U}\mathbf{Z}\mathbf{w}\right)\right\|^2. \end{aligned} \tag{102}$$

It follows that

$$\text{ISL} = \frac{\left\|\mathbf{R}^{1/2}\left(\mathbf{s}+\mathbf{U}\mathbf{Z}\mathbf{w}\right)\right\|^2}{\|\mathbf{s}\|^4}. \tag{103}$$

Next we note that

$$\mathbf{Z}\mathbf{w} = \left[\begin{array}{ccc} w_1\mathbf{I} & \cdots & w_{\tilde{M}}\mathbf{I} \end{array}\right] \left[\begin{array}{c} \text{col}_1(\mathbf{Z}) \\ \vdots \\ \text{col}_{\tilde{M}}(\mathbf{Z}) \end{array}\right] \stackrel{\triangle}{=} \mathbf{B}^*\tilde{\mathbf{z}}, \tag{104}$$

where $\{w_m\}$ are the elements of $\mathbf{w}$, and $\{\text{col}_m(\mathbf{Z})\}$ denote the columns of $\mathbf{Z}$. We can see from (104) that ISL depends on $\tilde{\mathbf{z}}$ only through the component of this vector that lies in the range space of $\mathbf{B}$. Therefore, for the study of ISL, it is sufficient to consider vectors $\tilde{\mathbf{z}}$ of the form:

$$\tilde{\mathbf{z}} = \mathbf{B}\boldsymbol{\xi}, \tag{105}$$

where $\boldsymbol{\xi}$ is an arbitrary $(2M+N-1)\times 1$ vector. Insertion of (105) into (103) and utilization of the fact that $\mathbf{B}^*\mathbf{B} = \mathbf{I}$ give:

$$\text{ISL} = \frac{\|\mathbf{R}^{1/2}(\mathbf{s}+\mathbf{U}\boldsymbol{\xi})\|^2}{\|\mathbf{s}\|^4}. \tag{106}$$

However, this is precisely the expression of ISL corresponding to the IV vector case; indeed, making use of (76), we have that: $\text{ISL} = \|\mathbf{R}^{1/2}(\mathbf{s}+\mathbf{U}\mathbf{z})\|^2/\|\mathbf{s}\|^4$. With this observation, the proof of the fact that an IV matrix filter cannot produce smaller values of either ISL or ISNR is concluded.

ACKNOWLEDGEMENT

We would like to thank Dr. Yu. Abramovich for bringing the rich Russian literature on the topic of this paper to our attention.

REFERENCES

[1] Y. I. Abramovich and M. B. Sverdlik, "Synthesis of a filter which maximizes the signal-to-noise radio under additional quadratic constraints," *Radio Engineering and Electronic Physics*, vol. 15, pp. 1977–1984, November 1970.

[2] V. T. Dolgochub and M. B. Sverdlik, "Generalized γ-filters," *Radio Engineering and Electronic Physics*, vol. 15, pp. 147–150, January 1970.

[3] V. M. Koshevoy and M. B. Sverdlik, "Effect of memory and pass band of a generalized filter on efficiency of noise suppression," *Radio Engineering and Electronic Physics*, vol. 18, pp. 1181–1188, August 1973.

[4] S. D. Blunt and K. Gerlach, "Adaptive pulse compression via MMSE estimation," *IEEE Transactions on Aerospace and Electronic Systems*, vol. 42, pp. 572–584, April 2006.

[5] V. P. Ipatov, "Choice of periodic PSK signal and filter combination," *Radio electronics and communications systems*, vol. 21, no. 4, pp. 60–67, 1978.

[6] V. P. Ipatov, V. I. . Korniyevskiy, V. D. Platonov, and I. M. Samoylov, "Minimum sidelobe level of a periodic discrete signal in a wide finite Doppler band," *Radio Engineering and Electronic Physics*, vol. 29, pp. 32–37, February 1984.

[7] J. Jedwab, "A survey of the merit factor problem for binary sequences." *Sequences and Their Applications – SETA 2004,* T. Helleseth, D. Sarwate, H. Y. Song, and K. Yang, Eds., vol. 3486, Lecture Notes in Computer Science, pp. 30–55. Springer-Verlag, Heidelberg, 2005.

[8] T. Høholdt, "The merit factor problem for binary sequences." *Applied Algebra, Algebraic Algorithms and Error-Correcting Codes,* M. Fossorier, H. Imai, S. Lin, and A. Poli, Eds., vol. 3857, Lecture Notes in Computer Science, pp. 51–59. Springer-Verlag, Heidelberg, 2006.
[9] N. Levanon, "Cross-correlation of long binary signals with longer mismatched filters," *IEE Proceedings - Radar, Sonar, and Navigation*, vol. 152, pp. 377–382, December 2005.
[10] C. Nunn, "Constrained optimization applied to pulse compression codes, and filters," *IEEE International Radar Conference,* Arlington, VA, USA, pp. 190–194, 9-12 May 2005.
[11] J. M. Baden and M. N. Cohen, "Optimal peak sidelobe filters for biphase pulse compression," *IEEE International Radar Conference,* Arlington, VA, USA, 7-10 May 1990.
[12] K. R. Griep, J. A. Ritcey, and J. J. Burlingame, "Poly-phase codes and optimal filters for multiple user ranging," *IEEE Transactions on Aerospace and Electronic Systems*, vol. 31, pp. 752–767, April 1995.
[13] R. C. Daniels and V. Gregers-Hansen, "Code inverse filtering for complete sidelobe removal in binary phase coded pulse compression systems," *IEEE International Radar Conference,* Arlington, VA, USA, 9-12 May 2005.
[14] S. D. Blunt, K. J. Smith, and K. Gerlach, "Doppler-compensated adaptive pulse compression," *IEEE Conference on Radar,* Verona, NY, USA, 24-27 April 2006.
[15] M. H. Ackroyd and F. Ghani, "Optimum mismatched filters for sidelobe suppression," *IEEE Transactions on Aerospace and Electronic Systems*, vol. 9, pp. 214–218, March 1973.
[16] S. Zoraster, "Minimum peak range sidelobe filters for binary phase-coded waveforms," *IEEE Transactions on Aerospace and Electronic Systems*, vol. 16, pp. 112–115, January 1980.
[17] R. Sato and M. Shinriki, "Simple mismatched filter for binary pulse compression code with small PSL and small S/N loss," *IEEE Transactions on Aerospace and Electronic Systems*, vol. 39, pp. 711–128, April 2003.
[18] C. A. Stutt and L. J. Spafford, "A 'best' mismatched filter response for radar clutter discrimination," *IEEE Transactions on Information Theory*, vol. 14, pp. 280–287, March 1968.
[19] Y. I. Abramovich and M. B. Sverdlik, "Synthesis of filters maximizing the signal-to-noise ratio in the case of a minimax constraint on the sidelobes of the cross-ambiguity function," *Radio Engineering and Electronic Physics*, vol. 16, pp. 253–258, February 1971.
[20] Y. I. Abramovich, "Estimation of accuracy of a method for synthesis of filters which optimize the cross-ambiguity function in accordance with the minimax criterion," *Radio Engineering and Electronic Physics*, vol. 18, pp. 785–787, May 1973.
[21] P. Stoica, J. Li, and M. Xue, "On sequences with good correlation properties: A new perspective," *The 2007 IEEE Information Theory Workshop on Information Theory for Wireless Networks,* Bergen, Norway, 1-6 July 2007.
[22] W. D. Rummler, "A technique for improving the clutter performance of coherent pulse train signals," *IEEE Transactions on Aerospace and Electronic Systems*, vol. 3, pp. 898–906, November 1967.
[23] D. F. DeLong and E. M. Hofstetter, "On the design of optimum radar waveforms for clutter rejection," *IEEE Transactions on Information Theory*, vol. 13, pp. 454–463, July 1967.
[24] L. J. Spafford, "Optimum radar signal processing in clutter," *IEEE Transactions on Information Theory*, vol. 14, pp. 734–743, September 1968.
[25] J. Li, P. Stoica, and Z. Wang, "Doubly constrained robust Capon beamformer," *IEEE Transactions on Signal Processing*, vol. 52, pp. 2407–2423, September 2004.
[26] P. Stoica and R. L. Moses, *Spectral Analysis of Signals*. Upper Saddle River, NJ: Prentice-Hall, 2005.
[27] J. D. Wolf, G. M. Lee, and C. E. Suyo, "Radar waveform synthesis by mean-square optimization techniques," *IEEE Transactions on Aerospace and Electronic Systems*, vol. 5, pp. 611–619, July 1969.
[28] S. M. Sussman, "Least-square synthesis of radar ambiguity functions," *IEEE Transactions on Information Theory*, vol. 8, pp. 246–254, April 1962.
[29] V. M. Koshevoy and M. B. Sverdlik, "Joint optimization of signal and filter in the problems of extraction of signals from interfering reflections," *Radio Engineering and Electronic Physics*, vol. 20, pp. 48–56, September 1975.
[30] V. T. Dolgochub and M. B. Sverdlik, "Synthesis of signals for optimization of the ambiguity function in a given region," *Radio Engineering and Electronic Physics*, vol. 14, pp. 1563–1566, October 1969.
[31] V. P. Ipatov and B. V. Fedorov, "Regular binary sequences with small losses in suppressing sidelobes," *Radio electronics and communications systems*, vol. 27, no. 3, pp. 29–34, 1984.
[32] Y. I. Abramovich, B. G. Danilov, and A. N. Meleshkevich, "Application of integer programming to problems of ambiguity function optimization," *Radio Engineering and Electronic Physics*, vol. 22, pp. 48–52, May 1977.
[33] D. E. Vakman, *Sophisticated Signals and the Uncertainty Principle in Radar*. New York: Springer-Verlag, 1968.
[34] V. P. Ipatov, V. I. Korniyevskiy, V. D. Platonov, and I. M. Samoylov, "Boundaries of the sidelobes of a periodic discrete signal in a broad Doppler band," *Radio Engineering and Electronic Physics*, vol. 29, pp. 25–32, February 1984.
[35] H. D. Schotten and H. D. Lüke, "On the search for low correlated binary sequences," *AEU – International Journal of Electronics and Communications*, vol. 59, no. 2, pp. 67–78, 2005.
[36] S. D. Blunt and K. Gerlach, "Adaptive pulse compression repair processing," *IEEE Conference on Radar,* Verona, NY, USA, 9-12 May 2005.
[37] M. Lobo, L. Vandenberghe, S. Boyd, and H. Lebret, "Applications of second-order cone programming," *Linear Algebra and its Applications, special issue on linear algebra in control, signals and image processing*, pp. 193–228, November 1998.
[38] J. F. Sturm, "Using SeDuMi 1.02, a MATLAB toolbox for optimization over symmetric cones," *Optimization Methods and Software Online*, vol. 11-12, pp. 625–653, Oct. 1999. Available: http://www2.unimaas.nl/ sturm/software/sedumi.html.

[39] J. Löfberg, "YALMIP: A toolbox for modeling and optimization in MATLAB," *The 2004 IEEE International Symposium on Computer Aided Control Systems Design,* Taipei, Taiwan, pp. 284–289, September 2004. Available from `http://control.ee.ethz.ch/~joloef/yalmip.php`.

TABLE I

THE SEQUENCES $\mathbf{s}_2$ USED IN $\mathbf{x}_3$ AND $\mathbf{x}_4$.

N	M	$\mathbf{s}_2$
16	0	$---++--+-+-+-$ $------++--+-+-+$
	20, 40, 60, 80.	$-------++--+-+-+$ $------++--+-+-+-$
21	0	$-------++++--+--+-+-+$ $------++-+--+-+-+-+$
	20, 40, 60, 80.	$--------++--+--+-+-+-$ $-------++-+--+-+-+-+$

TABLE II

THE SEQUENCES $\mathbf{s}_3$ USED IN $\mathbf{x}_5$.

N	M	$\mathbf{s}_3$
16	60	$--+-+----++--++$ $+--+-+--+-+-----+$
	80	$-------++--+-+-+-+$ $------++--+-+-+-+-$
21	60,80	$------++-+--+-+-+-+-$

TABLE III

THE SEQUENCES $\mathbf{s}_4$ USED IN $\mathbf{x}_7$ AND $\mathbf{x}_8$, FOR $\Phi = 5^\circ$.

N	M	$\mathbf{s}_4$
16	0	$---++--+-+-+-$ $------++--+-+-+-+$
	20, 40, 60, 80.	$-------++--+-+-+-+$ $------++--+-+-+-+-$
21	0	$-------++++--+--+-+-+-+$ $------++-+--+-+-+-+-+$
	20, 40,	$--------++--+--+-+-+-+$ $-------++-+--+-+-+-+-$
	60, 80.	$----------+-++++--+++$ $-+--+--+----+-+-+-+-+$

TABLE IV

THE SEQUENCES $\mathbf{s}_5$ USED IN $\mathbf{x}_9$, FOR $\Phi = 5^\circ$.

N	M	$\mathbf{s}_5$
16	60,80	$--+-+-----+--++$ $+--+++--+-+----+$
21	60,80	$---++++-+++-+-+-++-$ $--++++-----+-+--+-$

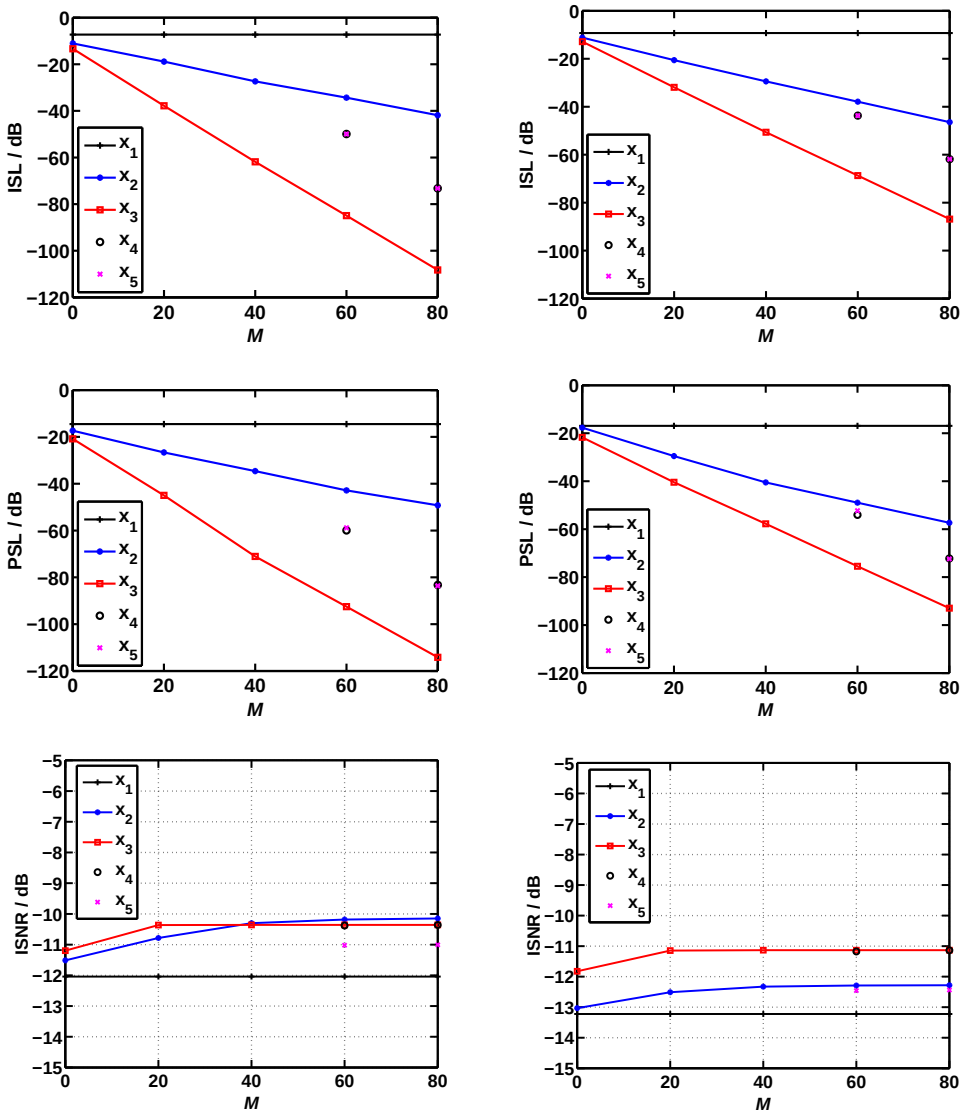

$N = 16$ $N = 21$

Fig. 1. The ISL, PSL, and ISNR metrics associated with designs $\mathbf{x}_1 - \mathbf{x}_5$, as functions of M, for both N=16 and N=21.

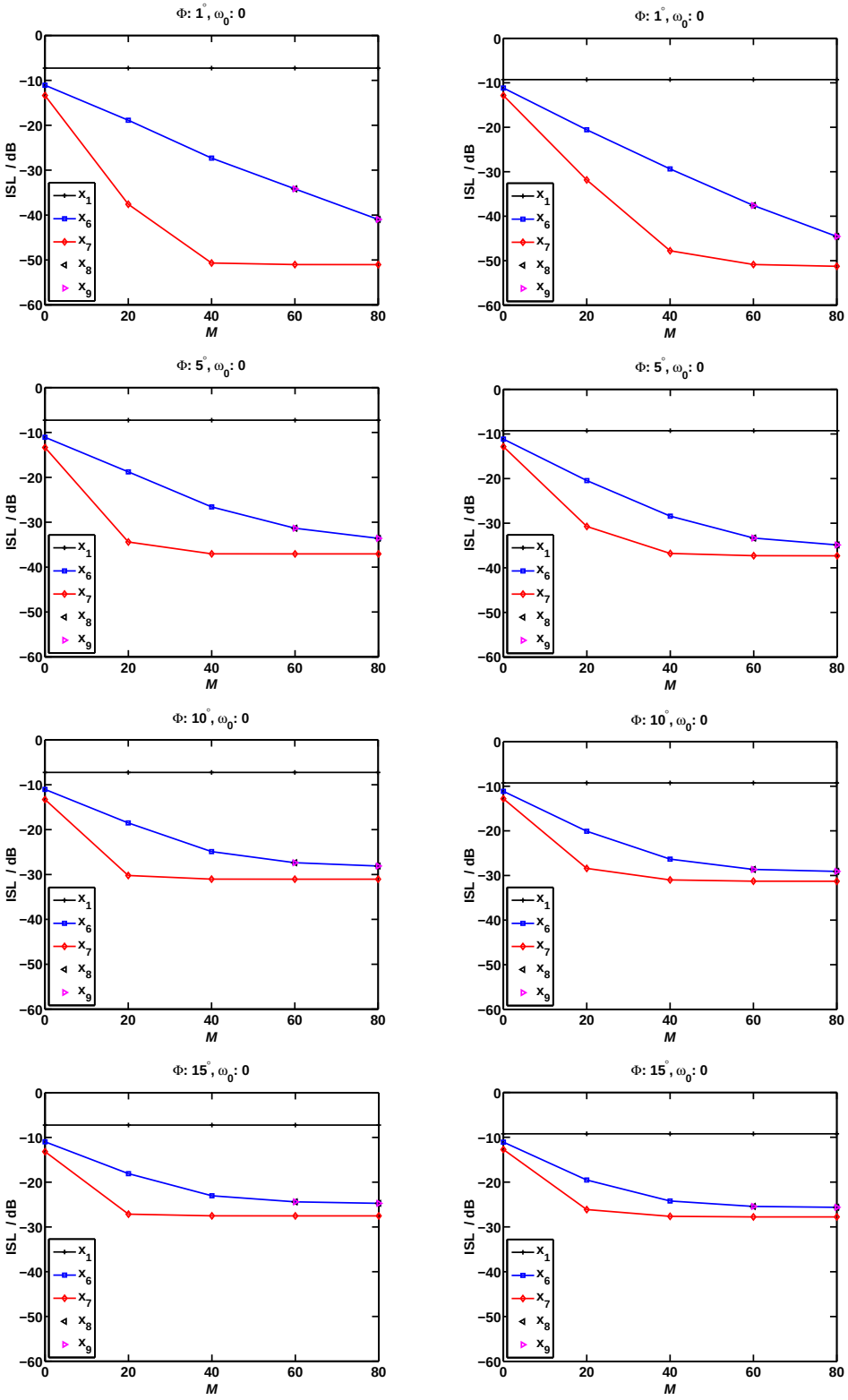

$N = 16$ $N = 21$

Fig. 2. The $\mathrm{ISL_D}$ metrics associated with designs $\mathbf{x}_1$, $\mathbf{x}_6$, $\mathbf{x}_7$, $\mathbf{x}_8$ and $\mathbf{x}_9$ for $\Phi = 1^\circ$, 5°, 10° and 15° and for both $N = 16$ and $N = 21$.

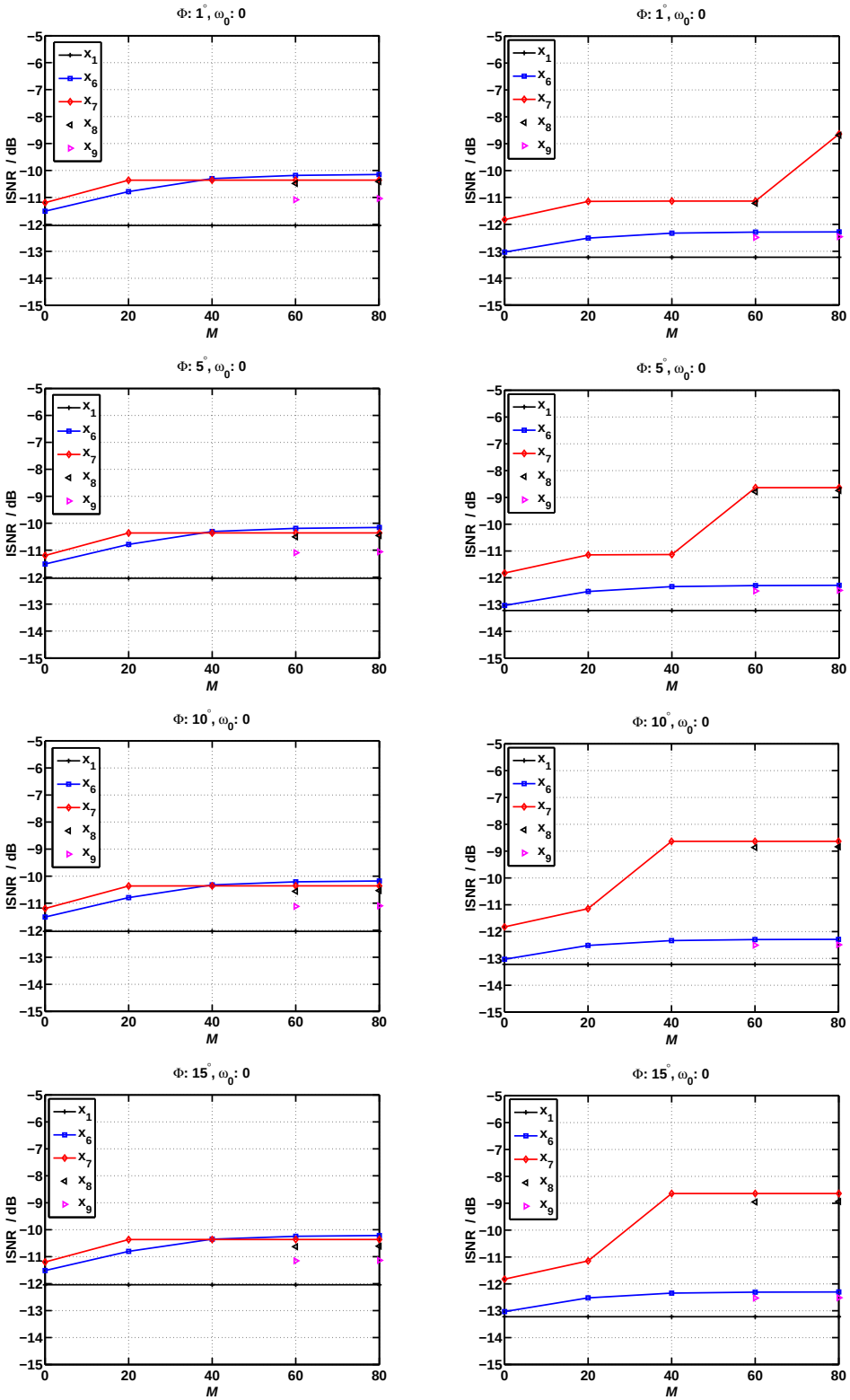

$N = 16$ $N = 21$

Fig. 3. The ISNR_{D} metrics associated with designs $\mathbf{x}_1$, $\mathbf{x}_6$, $\mathbf{x}_7$, $\mathbf{x}_8$ and $\mathbf{x}_9$ for $\Phi = 1^\circ$, 5°, 10° and 15° and for both $N = 16$ and $N = 21$.

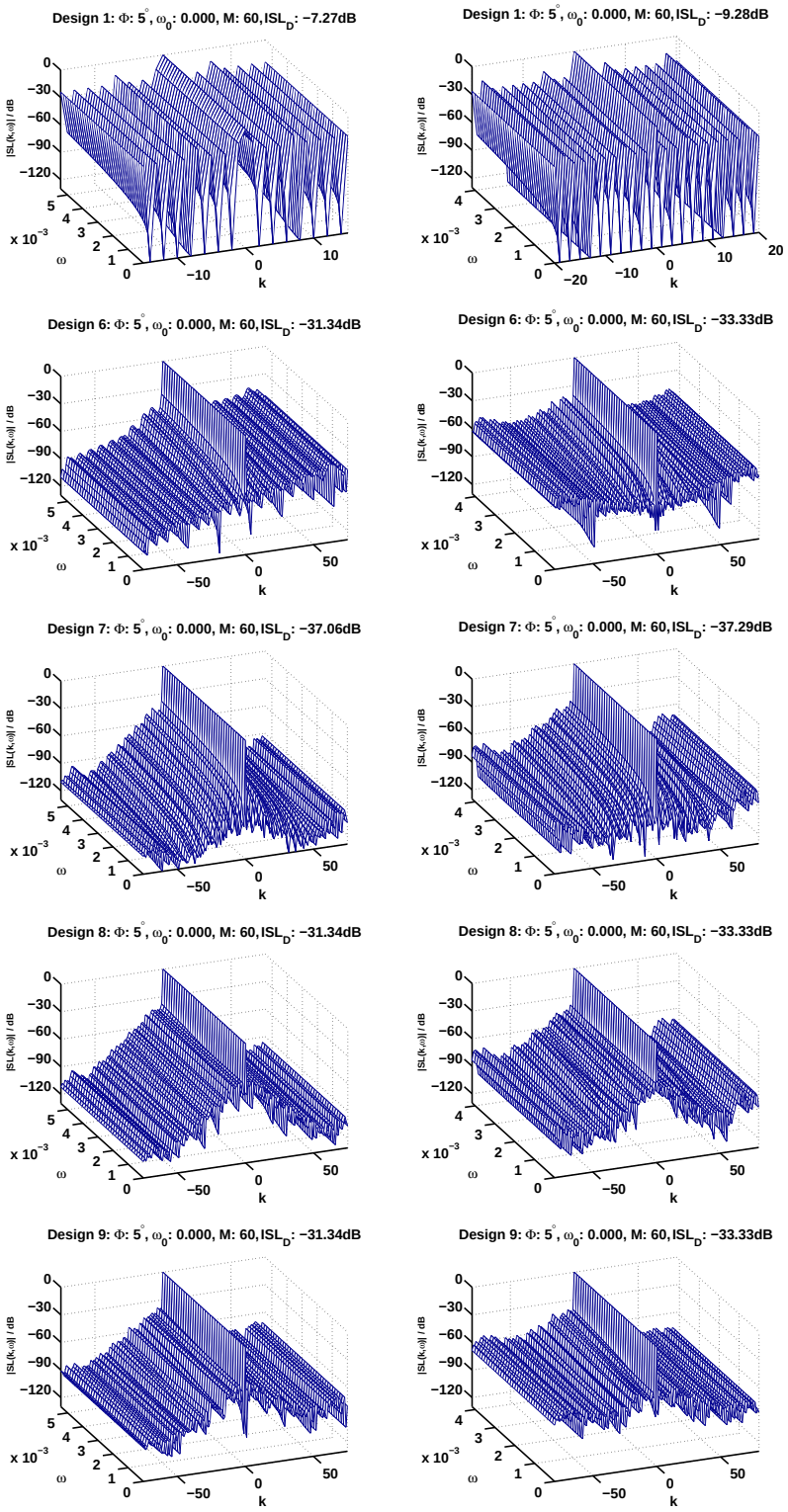

Fig. 4. The cross-ambiguity functions SL(k,ω), associated with designs $\mathbf{x}_1$, $\mathbf{x}_6$, $\mathbf{x}_7$, $\mathbf{x}_8$ and $\mathbf{x}_9$, for $\Phi = 5^\circ$, M=60 and for both N=16 and N=21. Note that for $\mathbf{x}_1$ we have SL(k,ω)=0 for $|k| \geq N$. Note also that to improve the visibility of the plots around ω=0, we show them only for $\omega \in [0, \Delta\omega]$ (the behavior for $\omega \in [0, -\Delta\omega]$ is similar).

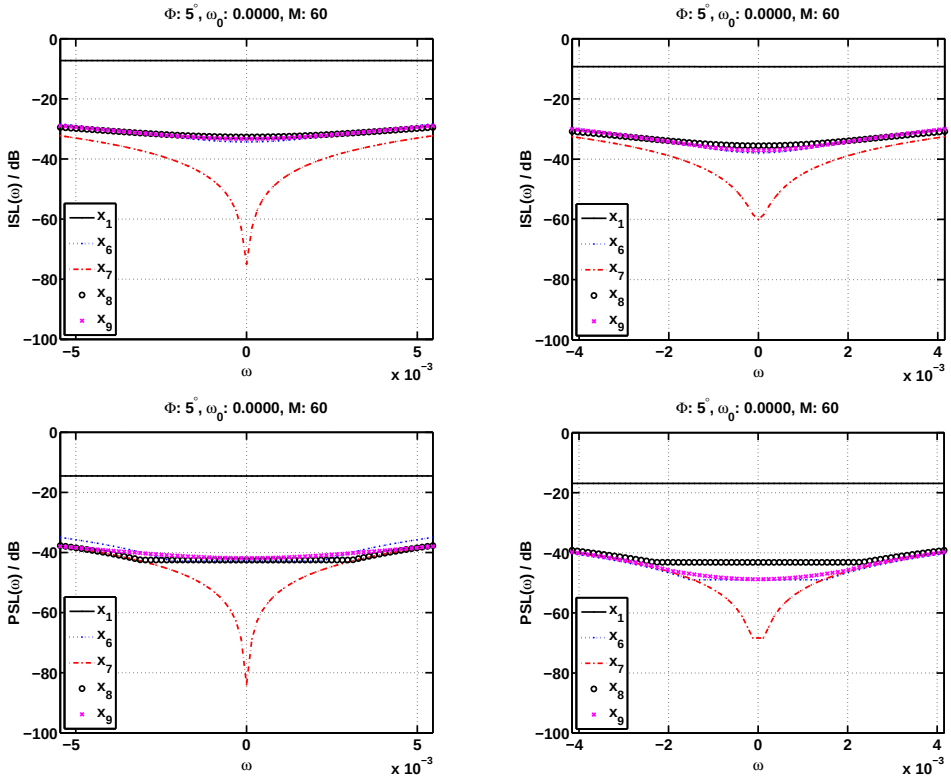

Fig. 5. The ISL(ω) and PSL(ω) metrics, associated with the designs $\mathbf{x}_1$, $\mathbf{x}_6$, $\mathbf{x}_7$, $\mathbf{x}_8$ and $\mathbf{x}_9$, for $\Phi = 5^\circ$, $M = 60$, and for both $N = 16$ and $N = 21$.